Hydrothermal Synthesis Of $CuMnO_2$ for Supercapacitor Applications

A thesis submitted towards partial fulfilment of the requirements for the degree of

Master of Technology in Nano Science & Technology

Roll Number: 002030701001

Examination Roll No.: M4NST22001

Registration Number: 154570

Submitted by

ARKA SEN

Under the guidance of

DR. CHANDAN KR. GHOSH

School of Materials Science & Nanotechnology

Jadavpur University

Course affiliated to

Faculty of Engineering and Technology

Jadavpur University

Kolkata-700032

India

2020-2022

M.Tech in Nano Science & Technology

Course affiliated to

Faculty of Engineering and Technology
Jadavpur University
Kolkata, India

CERTIFICATE OF RECOMMENDATION

This is to certify that the thesis entitled

"HYDROTHERMAL SYNTHESIS Of $CuMnO_2$ FOR SUPERCAPACITOR APPLICATIONS"

is a bonafide work carried out by Arka Sen under my supervision and guidance for partial fulfilment of the requirement of **Master of Technology in Nano Science & Technology** in **School of Materials Science & Nanotechnology**, during the academic session 2020-2022.

Dr. CHANDAN KUMAR GHOSH
Thesis Advisor,
School of Materials Science ,
& Nanotechnology
Jadavpur University,
Kolkata-700032.

Dr. SOURAV SARKAR Director,
Associate Professor,
School of Materials Science,
& Nanotechnology
Jadavpur University,
Kolkata-700032.

DEAN -FISLM
Jadavpur University
Kolkata-700032.

M.Tech in Nano Science & Technology

Course affiliated to

Faculty of Engineering and Technology
Jadavpur University
Kolkata, India

CERTIFICATE OF APPROVAL

This foregoing thesis is hereby approved as a credible study of an engineering subject carried out and presented in a manner satisfactorily to warranty its acceptance as a prerequisite to the degree for which it has been submitted. It is understood that by this approval the undersigned do not endorse or approve any statement made or opinion expressed or conclusion drawn therein but approve the thesis only for purpose for which it has been submitted.

Committee of final examination for evaluation of Thesis

1. _____

2. _____

3. _____

4. _____

DECLARATION OF ORIGINALITY AND COMPLIANCE OF ACADEMIC ETHICS

I hereby declare that this thesis contains literature survey and original research work by the undersigned candidate, as part of his Master of Technology in Nano Science & Technology studies during academic session 2020-2022.

All information in this document has been obtained and presented in accordance with academic rules and ethical conduct.

I also declare that, as required by this rules and conduct, I have fully cited and referred all material and results that are not original to this work.

NAME: ARKA SEN

EXAMINATION ROLL NUMBER: M4NST22001
CLASS ROLL NUMBER: 002030701001
REGISTRATION NO.: 154570 of 2020-2021

THESIS TITLE: Hydrothermal Synthesis Of $CuMnO_2$ for Supercapacitor Applications

SIGNATURE: DATE:

Dedicated to My Parents
&
My Professors

ACKNOWLEDGEMENT

The completion of any work successfully is not the credit of the sole person doing it. It requires the collective effort of a group people related to the work. In this regard, for the successful completion of my thesis work, I would like to thank the following persons. First of all, I would like to express my sincere gratitude to my thesis supervisor Dr. Chandan Kr. Ghosh, Director, School of Materials Science & Nanotechnology, Jadavpur University, Kolkata for his constant academic and moral support, guidance and ideas without which completion of this thesis would have been impossible. His motivations and academic lessons have helped me to think dynamically about the project and has helped me to complete the project successfully. I would like to thank all the faculty members of School of Materials Science & Nanotechnology, Jadavpur University, Kolkata, for giving me academic guidance throughout my M.Tech course in different subjects, the cumulative knowledge of which has helped me to complete the thesis work more effectively. I give my heartiest thanks to Dr. Dipten Bhattacharya, Senior Scientist, Central Glass and Ceramic Research Institute, for letting me access special characterization instruments specific to my project. Next, I wish to express my sincere thanks to Tanmoy Mondal, Pritam Mandal, Nibedita Halder and all other members of the Nanoscience Lab, School of Materials Science & Nanotechnology, for their timely support and guidance without which I could not have successfully completed the thesis. Next, I express my thanks to Mr. Pankaj Kr. Bhadra, from school of Materials Science & Nanotechnology for carrying out the general characterization of my sample that led to the timely completion of my thesis. Most importantly I would like to extend my sincere thanks to Sudipta Goswami, Department of Materials Science & Nanotechnology, Jadavpur University for her guidance & constant support. I would also like to sincerely thank my family for their moral support throughout the duration of the project.

INDEX

List of Figures

List of Tables

Abstract

In our work, we prepared $CuMnO_2$ through hydrothermal method. During this process, we changed NaOH concentration. These concentration were 3.4, 4.4 and 5.4g.The temperature during this process was set to 160°C.The duration of this process was 24 hrs. Different types of characterization were done such as XRD, FESEM, EDX, UV, PL, FTIR, CV, GCD. Through XRD we confirmed the prepared sample was $CuMnO_2$. After confirmation we checked morphology of three samples and change in morphology with NaOH variation. Once again we confirmed if there was any impurity in samples through EDX. It also helped us to check Cu, Mn and O concentration ratio. FTIR was used to checked the bonds present in all three samples. These bonds matched with reference papers. Ultraviolet Spectroscopy (UV), Photoluminescence Spectroscopy (PL) were used to find its optical property. These samples showed optical property in visible light range. From UV band gaps were calculated for all three samples and increase in band gap was noticed with increasing NaOH concentration. CV and GCD were used to find specific capacitance of all three samples. The calculated specific capacitance from CV matched with specific capacitance from GCD. It was seen that the sample with 4.4g NaOH concentration had the highest specific capacitance. From this we understood that these samples are applicable for supercapacitor application.

Chapter 1

Introduction

According to the International Organization for Standardization (i.e. ISO), Nanomaterial is defined as the 'material with any external dimension in the nanoscale or having internal structure or surface structure in the nanoscale', with nanoscale defined as the 'length range approximately from 10^{-9} to $100 * 10^{-9}$ meter'. The nanoscale is comparable to atoms and molecules. Nanomaterials show completely different characteristics compared to the same material at bulk form because of its microscopic dimension. Nanomaterials produce strong , highly conductive and chemically active elements. The technology used to create nanomaterials is known as *NanoTechnology*.

Nanomaterials have wide range of industrial applications. In sports industry, carbon nanotubes are used to create baseball bats. Baseball bats produced from nanomaterials are very light in weight. As a result of this, it improves the performance of players. In cosmetic industry mineral nanoparticles like titanium oxide are used as sunscreen which provides protection to the skin from ultra violet ray.

We specifically focus on the use of nano materials for building energy storage devices in this thesis. Energy storage devices are very essential for modern days to fight against lack of non-renewable elements. To solve this problem, we have batteries and capacitors. But both of these has certain advantages and disadvantages. Batteries can charge for longer time, but it has very slow charging and discharging speed. Capacitors has fast charging and discharging speed, but it can store charge for very less amount of time.

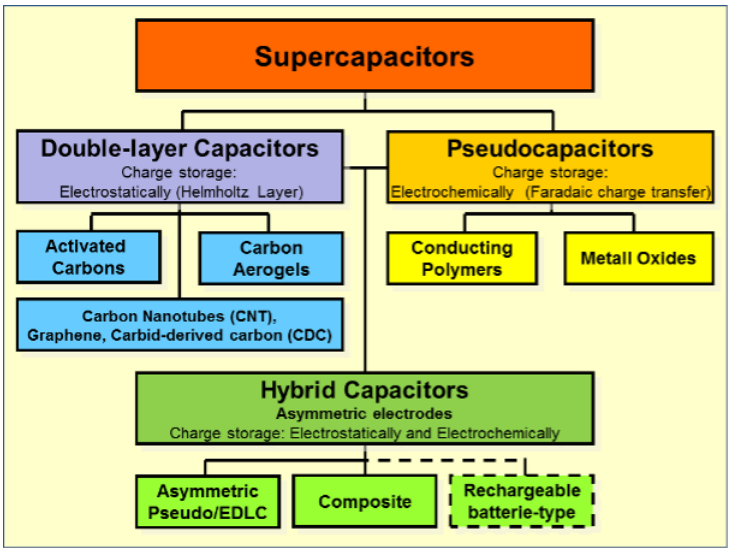

Figure 1.1: Different Types of SuperCapacitors.

Supercapacitor is the device which combine both advantages of the devices. For this reason there is a huge interest among researchers to find material which can be used to supercapacitor to surpass both battery and capacitor in the field of energy storage device.

Electrical energy is stored in supercapacitors via two storage principles, static double-layer capacitance and electrochemical pseudocapacitance; and the distribution of the two types of capacitance depends on the material and structure of the electrodes. Capacitors can be broadly categorized into three categories based on their storage principles. They are as follows.

- **Double-layer capacitor (EDLCs):** with activated carbon electrodes or derivatives with much higher electrostatic double-layer capacitance than electrochemical pseudocapacitance
- **Pseudocapacitor:** with transition metal oxide or conducting polymer electrodes with a high electrochemical pseudocapacitance.
- **Hybrid Capacitor:** With asymmetric electrodes, one of which exhibits mostly electrostatic and the other mostly electrochemical capacitance, such as lithium-ion capacitors.

Because double-layer capacitance and pseudocapacitance both contribute inseparably to

the total capacitance value of an electrochemical capacitor, a correct description of these capacitors only can be given under the generic term. The concepts of supercapattery and supercabattery have been recently proposed to better represent those hybrid devices that behave more like the supercapacitor and the rechargeable battery, respectively.

In order to increase specific capacity and cycle limit we change the morphology of electrode material. In recent we found some breakthrough by using mixed material of low cost transition material or metal oxide of transition metal. For instance, uniform porous $NiCo_2O_4$ nanoparticles obtained through a co-precipitation manifests a superior specific capacitance of 726 F g-1 at 1 A g-1 and a better cycle stability of 73% retention at 5 A g-1 after 2000 cycles. These transition metal provide greater surface area of electrode . It also reduces the distance between electrodes.

Among all the material delafossite materials are found most suitable material for energy storage. The chemical formula of delafossite material is ABO_2. Here A and B are both metals. This material involve in redox reaction which produces more ions. Thus it increases charge storage capacity of the material. Among the delafossite material we used $CuMnO_2$. Like other delafossite material $CuMnO_2$ is a layered structure. Its edge consist of MnO_6 and two Cu^+ ions are at inter layer sites. $CuMnO_2$ can be used as photovoltaic device, carbon monoxide and nitrous oxide removal agent. For creating low cost super capacitor we use hydrothermal process to synthesis $CuMnO_2$. Obtained $CuMnO_2$ nanoparticles used for both positive and negative electrodes of quasi-solid-state symmetric supercapacitor. Its electrochemical properties are investigated by cyclic voltammetry(CV), galvanostatic charged/discharged(GCD) and electrochemical impedance spectroscopy(EIS) techniques. After long-term cycle testing we found it has high specific capacitance, impressive power density . These result shows that it has great value of electrode material of a supercapacitor.

Chapter 2

Literature Review

In this chapter we review existing literature related to our work. We can broadly categorize the our literature review into four sections. They are a) review of delafossite materials as supercapacitors, b) general strategy of nanomaterial synthesis methodology c) characterization of nanomaterials and d) the use of nano materials for energy storage. Each one of them is described as follows.

2.1 Delafossite Materials as Supercapacitors

In our work we have used $CuMnO_2$ for supercapacitor application. $CuMnO_2$ belongs to the delafossite material category.Some delafossite materials are often used for supercapacitor application. Hence we first review existing literature which has used delafossite materials for super capacitor application.In order to do this first we need to understand structure and chemical composition of delafossite material.

Delafossite compound group belongs to ternary oxide group with general formula of ABO_2. In this structure A and B are cations and O is an anaion. A has linear coordination with two oxygen ions and it is in $^{+}1$ oxidation state. Examples of materials which can be A cation are Palladium (Pd), Platinum (Pt), Cupper (Cu) and Silver (Ag). The example of B cations in ABO_2 can be a p block cation, transition metal cation (i.e. where d blocks are half filled) or rare earth material. Transition metal oxide attracts a lot of attention

due to their variety of physical phenomena which change due to temperature ,pressure or doping. Such examples are superconductivity of cuprates due to high Tc and high magnetoresistance observed in magnatates. ABO_2 is characterized by a layer of linearly coordinated A cations stacked between edge-shared octahedral layers (BO_6) [1]. The B cation materials in ABO_2 are at the edges of BO_6 octahedral plane. The B cation which is at the center of BO_6 octahedral plane has $^{+}3$ oxidation state. The layers of BO_6 are interlinked by linear $O-A-O$ [2] Depending on the orientation of each layer in stacking, the delafossite structure can form as one of two polytypes [3]. One of the arrangements can be by stacking alternative A layer at 180° with respect to each other and creating hexagonal 2H type. Other one is by alternative A layers are in same direction but offset from each other at three electrode sequence. Delafossite material form R3m spacing group due to stacking of monoatomic triangular layers.

Different delafossite material can have different application depending on their chemical composition.To understand these characteristic we first take $CuFeO_2$ to analysis its charecteristic.In $CuFeO_2$, Cu, Fe and O are in $1:1:2$ ratio. But the amount Fe can be slightly higher than Cu. From that we can say hematite (Fe_2O_3) is present in $CuFeO_2$ material. Due to the presence of wide and different chemical composition, we can assume it has different application. Some of these application are as conductive films and UV solar cell due to its P type semiconductor property.These properties also depend on structure of $CuFeO_2$ material.

Just like any other delafossite material $CuFeO_2$ has A cation along the c-axis and octahedral BO_6 layer is perpendicular to c-axis. Depending on layer stacking it will produce rhombohedra(3r) or hexagonal (2H) symmetry. For example, $CuFeO_2$ is constructed of two-dimensional copper cation linear bonding with oxygen and slightly distorted edge shared octahedral $Fe3^{+}O_6$. This structure depends on temperature, pressure etc. For example, $CuCrO_2$ under compression take the structure of rock salt. Due change in structure of delafossite material we can observe different electrical property and optical properties [1].

For properties like high electrical conductivity and high optical transparencies are specific characteristic which are very hard to find together in any material. Transparent conductive oxide(TCOs) are only materials in which these two characteristic are found together.These TCOs materials are devided in two types. Depending on electron or hole concentration in band gap of these material they are called n-type or p-type. The carrier concentration and band gap of these materials are $10^16 - 10^21\ cm^-3$ and $3eV$. N-type TCOs are used used for two application firstly for photovoltic cell,transparent electrode and secondly UV light emitting diode,gas sensor. Compare to that the p-type TCOs of similar properties are difficult to find. If we can find similar characteristics p-type material we can make a P-n junction device which will improve transparent electronic devices.But p-type TCO has failed to meet the requirement due to their low conductivity or transparency. Conductivity is directly proportional to carrier concentration and carrier mobility.High conductivity can be obtained by increasing carrier concentration or carrier mobilty or both. For n-type TCOs oxygen vacancy creates high carrier concentration. Another reason for high conductivity of n-type TCOs is high carrier mobility.When s-orbital of n-type TCOs goes to hybridisation with heavy metal cation it creates delocalization of electron and increases electron mobility.

Fleischer et al analysed optoelectronic property with synthesis temperature. From that analysis, he concluded that it is very hard to synthesis p-type TCOs with low cost synthesis process and improve optoelectronic property. Amid all these delafossite structure made a huge impact due to their interesting property and application in various field. These are ternary metal oxide with AMO_2 where A^+ and M^{3+} are monovalent and trivalent cation. A^+ cation has bond with two oxygen atoms and M^{3+} atom has bond with six oxygen atoms. In this structure there are layers of $M^{3+}O_6$ octahedra and these are perpendicular to c axis. Cation A^+ bonded with two oxygen atom creat a dumbell like structure which is parallel to c axis. $M^{3+}O_6$ octahedra is parallel to ab plane.Among Cu delafossite copper cromioum oxide($CuCrO_2$) considered as most promising material

since it has O^2- and Cr^{3+} covalent mixture and high concentration of 3d state of Cr near valence band maximum (VBM) and high band gap.Its optoelectrical property is tunable due to its structure which facile substitution with with aliovalent and or isovalent cations at the Cr site.It has low systhasis temperature and thermally stable in air.The $CuCrO_2$ has layers of octahedral CrO_6 which are perpendicular to c axis and Cr is in center of CrO_6 octahedral.Cr cation has a oxidation state of $^+3$. $CuCrO_2$ has two type of polytype one is hexagonal $\alpha - 2H$ polymorph and other one is rhombohedral $\alpha - 3R$. $CuCrO_2$ has relativly small a,c axes.For doped $CuCrO_2$ it has shown different length of a axis and length of c axis does not change much. For delafossite film it is seen the length of c axis changes due to change in average length of $Cu - O$. To understand supercapacitor application of $CuCrO_2$ which is prepared through Mg doping of 0,0.0.05,0.1,0.15 we need to understand its electrochemical property.Cyclic voltammetry(CV) test is done at scan rates of 5,10,20,30,40,50mV/s for 0-.4volt range to understand its electrochemical property and the samples are named as MT0,MT1,MT2,MT3 according to 0,0.05,0.1,0.15 Mg doping respectively.From the CV it was found that perfectly separable redox peak. It proved that each sample has different charge storage capacity.The CV curve also indicated that these samples showed a pseudo capacitance behaviour.As scan rates were increased the difference between charging and discharging peak also increased.The polarisation of electrodes increased with increasing scan rate. The area under CV curve increased with increasing scan rate for all samples.It was due to increase in charge transfer between electrodes.Further specific capacitances were calculated by equation below from CV curves.

$$Csp = \frac{\int id}{S\Delta Vm} \tag{2.1}$$

Csp is specific capacitance, $\int idV$ means integral area in CV curve,S is scan rate, ΔV is voltage window,m is active mass.The specific capacitances of MT0, MT1, MT2, MT3 were $93, 129, 149$ and 249 farad per gram (F/g).The specific capacitance of MT3 was highest among all four samples.Specific capacitance of MT3 sample was more than two times the specific capacitance of MT0. Also specific capacitance decreased with increasing scan rate

for all samples. For acquiring more information about supercapacitor application charge-discharge behaviour analysis was done for 1, 1.2, 1.4, 1.6, 1.8 ampere per gram (A/g) in 0 to 0.4v range.This curve also showed pseudo capacitance behaviour just like CV curve.The specific capacitance of MT3 was calculated from charge-discharge curve.The formula to calculate specific capacitance is given below-

$$Csp = \frac{I\Delta t}{m\Delta V} \tag{2.2}$$

Csp is specific capacitance, I is discharge current density, m is active mass, δV is potential widow, δt is discharge time.The specific capacitances for MT3 sample were $113, 101, 96, 88, 74$ F/g for $1, 1.2, 1.4, 1.6, 1.8$ A/g.As it was seen that specific capacitance of MT3 sample decreases with increasing current density.This conclution matched with CV conclusion. For supercapacitor application long cycle life is one of the important aspect.The MT3 sample showed cyclic stability for 2000 continuous cycle at $50mV/s$ scan rate.Specific capacitance value was increased at initial cycle.It might be due to presence of large no of charges of electrolyte and electrode.After that it maintained 92 percentage of initial value of specific capacitance even at 2000th cycle. From this,it could be said that MT3 sample showed significant potential as active electrode material. Electrochemical impedance spectroscopy(EIS) was performed and Nyquist plots were examined at frequency range of 100kHz to 10MHz.The intercept on real impedance axis represent resistance between electrode and electrolyte.It also correspond to series resistance of equivalent circuit.The semicycle at high frequency represented charge transfer resistance due to Faradic reaction between electrolyte and electrode.Lowest charge transfer resistance was seen in MT3 sample.From this it could be concluded that MT3 sample had highest conductivity among all samples[1a]. Just like $CuCrO_2$,$AgFeO_2$ also has electrochemical property which makes it suitable for supercapacitor application.In this paper four $AgFeO_2$ samples were prepared by varying calcination temperature.The samples were AFO-80, AFO-200, AFO-400, AFO-550 for uncalcinated, $200°C, 400°C, 550°C$ respectively. Initially CV and GCD were performed to understand electrochemical prop-

erty of all sample. CV was performed for 10mV/s scan rate at $0.1 - 0.9$ voltage range. Every samples showed pair of reversible peaks.It suggested pseudo capacitive behaviour for all samples.The pair of peaks were caused by transition of Fe^{3+} to Fe^{2+} at 0.8V and 0.25V.The integral area under CV curves of all samples showed large charge storage capacity.The area for AFO400 was largest among all samples.Thus AFO400 showed superior psudocapacitive behaviour. Specific capacitance calculated through the formula given below-

$$Cs = \frac{\int id}{2\Delta Vm} \tag{2.3}$$

Here Cs is specific capacitance,,S is scan rate,m is active mass,i is current,ΔV is voltage window.The electrochemical properties confirmed by GCD. GCD for all sample was done within 0.1 to 0.9 voltage range at $0.8A/g$ current density. The plot exhibited nonlinear charge-discharge behaviour.Longer discharge time could be seen in GCD plot. It symbolized better capacitance.The supercapacitors were calculated from GCD plot.The value of $AFO - 400$ was highest.The GCD curv could be devided in three parts.For discharge curve 0.1 to -0.7 had largest slop and -0.7 to 0.9v had smallest slop. The $-.7$ to 0.9v due to transformation of Fe^{2+} to Fe^{3+}. If scan rate was changed than it could be seen that specific capacitance decreases with increasing scan rate.At that time AFO400 showed highest specific capacitance among all samples. $CuMnO_2$ also has supercapacitor property. In this paper these properties were discussed. Electrochemical tests were done on $CuMnO_2$ with 4M KOH as electrolyte. CV test was done at $10, 30, 50, 60, 100$mV/s scan rates at $0 - .7$V range.It showed a pseudocapacitivebehaviour.For example anode peak and cathode peaks were found on 0.471V and 0.272V respectively for 10mV/s scan rate.It was because reverse redox reaction between $M - O$ or $M - OOH$(where M is Cu and Mn) with OH^- ion of electrolyte.There was slight shift of redox peaks due to polarisation and ohomic resistance with increasing scan rate.They also performed GCD test at current density of $5, 6, 8, 10, 12$A/g.The specific capacitance calculated from GCD curve decreases from 765 to 425F/g for 5 to 12A/g current desity.Specific capacitance remained 87.8 percentage even after 10000 cycles at 8A/g current density.

2.1.1 $CuMnO_2$ Nano Particles As Supercapacitor

The study in [4] prepared $CuMnO_2$ nanomaterial through low temperature hydrothermal method. At the time of preparation he used 15 mmol $Cu(NO_3)_23H_2O$ and 15 mmol $Mn(NO_3)_2H_2O$. These were dissolved in 70ml deionized water and $4.4g$ NaOH were mixed with solution. After that above solution was stored in 100 mL Teflon-lined autoclave. Then it was heated at 80°C for 24 hrs. Finally they got a reddish brown precipitate. It was washed by deionized water and ethanol. After drying it for 24 hr at 60°C they got $CuMnO_2$ nanomaterial. Similarly the work in [5] used 7.5 mmol of $Cu(NO_3)_23H_2O$ and 7.5 mmol of $MnCl_2.4H2O$ and dissolved it in 35 ml deionized water. Them $NaOH$ is added to the above solution. The mixture was stirred for 10 minutes. It was then sealed in 50 ml Teflon-lined autoclave and heated at $100°C$ for 24 hr. The autoclave cooled down to room temperature naturally.

After centrifugation and washing it several time with deionized water and ethanol and dried. In this experiment by varying NaOH quantity from 1g, 2g and 3g they created three sample of $CuMnO_2$ nanomaterial. The study in [6] took 0.15 g of CTAB added to 50 mL of mixture of deionized water and ethyl alcohol (1 : 1), and then 5 mL of NaOH (2 mol/L) mixed with the solution. 2.5 mL of $Mn(CH_3COO)_24H_2O$ (0.1 mol/L) solution, and 2.5 mL of $Cu(NO_3)_23H_2O$ (0.1 mol/L) were add to above solution. This solution stirred for 2hr to get a homogeneous solution. After that it was stored in five 100 ml Teflon-lined autoclaves. These autoclaves are heated at $140°C$,$160°C$,$180°C$,$200°C$, $220 \circ C$ respectively for 24 hours. The autoclaves are cooled down to room temperature. After that obtained powder centrifuged and washed several times with deionized water and ethanol. Finally, it was dried at $70°C$ for 12 hours. At the end of the process they got $CuMnO_2$ nanomaterial. The work in [7] prepared Mg doped $CuMnO_2$ by hydrothermal method. 15 mmol $Cu(NO_3)_23H_2O$, $15x$ mmol $Mg(NO_3)_24H_2O$,$(x = 0.05, 0.10)15(1-x)$ mmol $Mn(NO_3)_24H_2O$ were dissolved in 70 ml deionized water at room temperature and 4.4 g of NaOH was added to above solution. This solution was stirred for $10 - 30$ min to get a homogeneous solution. This solution was poured and sealed in 100ml Teflon-lined

autoclaves and heated at 80°C for 24 hours. The obtained reddish-brown precipitate washed with deionized water and ethanal. The obtained powder of Mg doped $CuMnO_2$ dried at 60°C for 12 hours. The study in [8] used $Cu(NO_3)_2 3H_2O$ and $Mn(NO_3)_2 4H_2O$ (15.0 mmol of each) and dissolved in 70 ml of distilled water. 4.4g of NaOH was mixed with 20 ml distilled water and added with above solution. It was stirred for 15 min.This solution was poured in autoclave and heated at 80°C for 24 hours. This reddish-brown precipitate was washed through distilled water and ethanol. After that it was dried at 55°C for 8 h. At the end of this process they got $CuMnO_2$ nanomaterial. In [9] they used 15 mMol $Cu(NO_3)_2 3H_2O$ and 15 mMol $Mn(NO_3)_2$ and dissolved in 70 mL deionized water at room temperature. The above solution was mixed with 4.4 g of NaOH. This solution stirred for 15 min and stored in 100ml Teflon-line autoclave at 80°C for 24 hours. After 24 hours they got reddish brown precipitate washed with deionized water and absolute alcohol for several times and stored in absolute alcohol solution. The work in [10] first dissolved 3.5 mmol $Mn(NO_3)_2 4H_2O$ and 3.5 mmol $Cu(NO_3)_2 3H_2O$ dissolved in 30 ml H_2O. Then 2.2 g $NaOH$ was added to above solution and stirred for 30 min at room temperature. The mixture poured to the 50 mL, Teflon-lined stainless-steel reactor at 80°C for 24 hours. The obtained brown precipitate was sequentially washed with water and methanol. Lastly, the precipitate was dried at 60°C . Above we have discussed CuMnO2 nanoparticle preparation.These CuMnO2 nanoparticles have supercapacitor property.These properties can be analysed by CV,GCD.In this paper 4M KOH was taken to be used as electrolyte.First CV test was done at 10,30,50,60,100 mV/s scan rates.Two redox peaks were seen from CV curve.This implied that the sample had pseudo capacitive behaviour.For example two peaks were seen at 10mV/s.One was anode peak at .471V, other was cathode peak at .272V.These peaks resulted due to reverse redox reaction between M-OH or M-OOH(where M represent Cu and Mn) with OH^- ion of electrolyte.A slight seperation of redox peaks were noticed with increasing scan rate.It was due to polarisation and ohomic resistance increase during the process.The GCD curve was plotted for current density for 5,6,8,10 and 12 A/g.It showed nonlinear

behaviour.The calculated specific capacitances were 765 to 425 F/g for 5 to 12A/g current density.The specific capacitance(Cm) decreased with increasing scan rate.Above all 87 percentage of initial Cm remain even after 10000 cycles.To do further electrochemical investigation they did EIS.The Nyquist plot drown from EIS was straight line at low frequency and semicircle at higher frequency.The low frequency part was due to charge transfer between electrolyte and electode.The high frequency part was due to diffusion resistance. In this paper CV test was done on CuMnO2 at 0-0.5V for 5,10,20,50,100 mV/s scan rates.From the CV curves the redox peaks were identified clearly.IT proved the behaviour of pseudo capacitance.Especially for CuMnO2 crystal at 160°C the redox peaks could be seen more clearly than any other samples.The CV curve of CuMnO2 sample at 160°C had largest area under CV curve and highest peak current.So the capacitive ability of CuMnO2 at 160°C was highest.The GCD test was done for 1,2,5 and 10 A/g current density.For 1A/g specific capacitance of CuMnO2 at 160°C was 921A/g.During EIS they got a straight line for CuMnO2 at 160°C.It had highest slop at low frequency which meaned low diffusion resistance and better capacitive behaviour.The capacitance at 160°C remained 90.7 persentage of initial value after 1000 cycles.The reason for high capacitance at 160°C was nanowire type morphology which allowed large surface area and large charge transfer between electrode and electrolyte.

2.2 General Strategy of Nanomaterial Synthesis

2.2.1 Hydrothermal Synthesis

$CuMnO_2$ can be prepared by different synthesis method. Among all those methods hydrothermal synthesis is considered as common method. It is due to hydrothermal method is cost effective, required low reaction temperature. F.Wang and his co-workers has done hydrothermal synthesis on $CuMnO_2$ at $180°C$ for 24 hours and they got a nanostructure in range of $1 - 1.5$µm and thickness of 45 nm [11]. Dehua Xiong has prepared $CuMnO_2$ nanocrystal through hydrothermal process at only $80°C$ for 24 hr in 100 Ml Teflon au-

toclave [12]. There is another research done by Dehua Xiong on preparing $CuMnO_2$ nanoparticle where he used temperature from $80° - 160°$C for 24h Another researcher Maria Poienar and her co-workers prepared $CuMnO_2$ through hydrothermal method by varying temperature, PH. The precursors were weighted and mixed at desire proportion with distilled water. Then this mixture was stirred at room temperature until it becomes a homogeneous solution. After that it was stored in Teflon-lined stainless steel autoclaves volume of 29 ml or 49 ml. This autoclave was heated at $100°, 120°, 150°, 200°$ and different temperature such as $6, 12, 24, 60$ h. The PH of the solution changed through the NaOH variation [13]. In L.Wang paper he and his co-workers first mixed CTAB to deionized water and ethanol then they added NaOH. $Mn(CH_3COO)_2, 4H_2O$ and $Cu(NO_3)_2.3H_2O$ added to the above mixture. After stirred the solution for 3 hr, they sealed it in 100 ml Teflon-lined autoclave and heated it for 24 hr at 180°C. After washing it several time with ethanol and deionized water, they dried it at 70°C. In this way they got $CuMnO_2$ nanocrystal [14]. Q.Zhang in his paper also used hydrothermal method to produce $CuMnO_2$ at only 80°C. $Cu(NO_3)_2$, $Mn(NO_3)_2$ and $NaOH$ are mixed together with 70 ml water. This mixture then stirred for 15 minutes to create a homogeneous solution. This homogeneous solution is stored in 100 ml Teflon-lined autoclave and heated at 80°C. After that they got a reddish-brown precipitate. It is then washed with ethanol and deionized water. After drying they got powder like sample [12]. Siti Machmudah prepared ZrO_2 nanoparticle through hydrothermal method. For this they used stainless steel Teflon container and they stored 0.1 to 0.5 M concentration precursor solution. It was then heated 180°C for 12h. It was then washed through deionized water and ethanol and dried at 60°C for 6h. Lastly calcinated at 600°C for 6h [15]. Synthesis of inorganic material at temperature higher than 1000°C has disadvantage of not able to control size of material. There are also techniques like physical vapour deposition, chemical vapour deposition. But these methods are costlier than hydrothermal method and these require toxic precursors. So, these methods cannot be used for coating and film production. Hydrothermal method is done at a temperature which is higher than boiling temperature of solvent at a closed

container. It provides an advantage of choice of solvent, PH and reagent. It also helps to create nanocrystal without any need for any temperature increase during the process. But it also has disadvantage which is it require long reaction time. Another disadvantage of hydrothermal method is that if reagent and solvent are not chosen carefully particle size will increase [16]. Tadafumi Adschiri worked on hydrothermal synthesis of metal oxide. In this research he said that we need to know the solubility of crystal substance in high temperature water. To understand solubility we need to know equilibrium constant of reaction which is k. He also said that metal ion solubility depend on temperature and PH.For hydrothermal synthesis we need to know the optimum temperature and PH at which metal oxide will be soluble in water [17].

2.3 Characterization of Nano Materials

The study in [18] was XRD, SEM, Raman Spectrum , uv-vis , FTIR for CuMnO2 . XRD pattern for $CuMnO_2$ was done for $450°C$ to $900°C$.The 2θ range for this was 15 to 100 with $Cu\ K\alpha$ radiation at $\lambda = 0.154178$ nm. The pattern was compared with JCPDS cards. Particle size was analysed by particle size analyzer. Surface morphology was analysed by SEM. The voltage fixed at 20kv for SEM. Different bond present in $CuMnO_2$ identified by FTIR. Powder sample was used for FTIR. The sample was pressed in a disk before using in FTIR. The range of FTIR graph was 300 to $3900cm - 1$. Ramon spectrum was done on the powder sample in 300 to 1200nm range. The sample was excited by Ar^+ laser at 514.5nm. UV-VIS was done to find the energy band gap. From direct optical transition they found energy band gap. Conductivity was measured by two probe method using under argon atmosphere using an Agilent LCR meter 4363B. $CuMnO_2$ used as working electrode and KOH used as electrolyte. A conventional cell with Pt electrode (Tacussel) and a saturated calomel electrode (SCE), were used for the plot of the intensity potential J(V) curves. The work in [19] prepared $CuMnO_2$ at 623 to $1223k$. Each sample was examined by XRD plot. The particle size was also calculated by XRD plot. $CuK\alpha$ X-

ray powder diffraction ($\lambda = 0.154$ nm) used for XRD plot. From XRD plot we got a monoclinic structure with a lattice constant of $a = 0.5601$, $b = 0.2888$, $c = 0.5900$ nm, and $\beta = 103.98°$. From this XRD plot some impurity detected in Cu_2O peaks. The particle size from crystallite size distribution analysis was around 50 nm. In order to obtain single phase $CuMnO_2$ in air to examine the process TG-DTA measurement was carried out. In TG curve there was a decrease up to 500k due to dehydration. Sample mass increased after 550k and decreased significantly at 1200k.During dehydration Cu^+ ion valency changed from 1^+ to 2^+ and $Mn_2{}^+$ changed to Mn_3^+ and finally at Mn_4+ at $650k$. This confirmed MnO_2 presence. The significant decrease at $1200k$ was due transition from Cu_2^+ to Cu_1^+.

Based on above method an improved sintering process was suggested. In, the first step of this process the was annealed in air 623 K in order to obtain Cu_2^+ and Mn_3^+ by oxidation. In the second step annealed sample was calcinated in Ar to maintain a valence of Mn in 3 and reducing Cu valency at 1. By this a single phase $CuMnO_2$ was prepared. The diameter of $CuMnO_2$ was 64 nm after this process.

TEM image of improved $CuMnO_2$ was done at a range of 50 nm. Through SQUID magnetometer magnetization was measured at an external magnetic field of 50 to -50 kOe at temperatures of 5–300 K. Both field cooled and zero field cooled were found temperature dependent. At temperature above 200 k it behaved as paramagnetic material. At -580 k it behaved as antiferromagnetic. From we could say it behave according to Curie–Weiss law described in Equation 2.4.

$$\frac{1}{\chi} = \frac{(T - \theta)}{C} \tag{2.4}$$

According to this law, inverse magnetic susceptibility is proportional to temperature.

2.4 Use of Supercapacitors

During 1957 petrol become most credible energy source. At that time, Howard Becker at General Electric produced first supercapacitor as clean sustainable energy source. During

first several years it did not get any attention. In recent year it got more attention due to climate change. After the progress in material science , it opened many options for improving the limitation of supercapacitors. Based on materials supercapacitor such as electrostatic double-layer capacitance, electrochemical pseudocapacitance and hybrids could be designed. Graphene nanomaterial is considered as good supercapacitor material. Due to its large surface area, it has a very high capacitance. In order to achieve high specific capacitance we need electrode of large surface area and pore size appropriate to that surface area. For carbon it has a very high surface area. So it should provide specific capacitance around 200Fg -1 to 500Fg -1 . But it practically provides low value of specific capacitance. It is due large pore size distribution along its surface. Most of pore size is micropore size. This type of pore size is non-accessible by ions of most electrolytes. That is the reason activated carbon perform poorly as EDLC(electric double layer capacitor). CNT on the other hand has large surface area and high mesoporosity. Due to high mesoporosity it provides accessibility to ions of electrolytes. Due to this it can be used in EDLC and it provides large specific capacitance. Graphene also has same advantages as CNT as a supercapacitor material. Graphene is one atom more thickness than CNT. It provides more superior as supercapacitor than CNT [20]. Recently the need for better energy storage system has grown. Supercapacitor has proven very effective in field of energy storage devices. Supercapacitor has high power density, charging discharging speed and long cycle life. But it has low energy density compare to battery. Many researches are done in order to overcome this limitation. The supercapacitor energy is

proportional to square of applied voltage. In order to that we need electrolyte with high voltage window. To use high working voltage electrolyte we need electrode which is free of oxygen containing function such as COOH , OH and C=O because it will decompose the electrode material. CNT and graphene have special physical structure of sp 2 between carbon which reduce the resistance and increases conductivity. Due to free of surface-dangling bond it works perfectly as supercapacitor. CNT and graphene have high surface which helps it to reach higher specific capacitance [21]. According to

past researches it is seen that carbon is very good electrode for EDLC(electric double layer capacitor). As for, pseudocapacitors the material used for electrode are transition metal oxides such as MnO_2 ,RuO_2 ,Fe_2O_3 ,NiO and V_2O_5 . Recent research show that these metal oxides have higher capacitance compare to carbon. Among these metal oxides RuO 2 is very expensive metal oxide. So, we use Co_3O_4 like metal oxides which are cost effective and has good electronic conductivity. But Co_3O_4 has a drawback which due its poor cyclability. In order to improve this drawback Co_3O_4 nanomaterial is prepared by changing its morphology. Some times nitrogen and cadmium doping are used with support of nickel to improve its low cyclability. Even then, it still has the limitation of capacitance loss with progressing cycles and low power density. In order to improve that cobalt oxide and carbonaceous material are combined. Due to this, it can be used by EDLC and pseudocapacitor mechanism. Through three electrode method [22]. For supercapacitor surface area is an important factor. If we have a large surface area then it will help to improve specific capacitance. Electrode thickness is also an important factor for supercapacitor. If we decrease thickness of electrode material then it will in increase electrode material specific capacitance. Since specific capacitance is F/g. So, with decreasing material mass(g) the value of F/g increases. But contribution of electrode mass in overall cell specific capacitance reduces. To increase contribution of electrode material in overall cell specific capacitance we need to increase thickness of electrode. According to author Wang used graphene as electrode material for supercapacitor. First wang used graphene material without any nanoscale hole across its surface and increased electrode thickness by increasing material by four time it is seen that specific capacitance of material decreases by 50negatively on overall specific capacitance. For second case wang used graphene with nanoscale holes across its surface and thickness of electrode increased by four times material. It showed that specific capacitance of material decreased by just 12.5% and did not affect significantly to overall specific capacitance. It proved that electrolytes could access pores due to nanoscale holes. The contribution of electrode material in overall specific capacitance increased [23]. Nowadays transient metal oxide

nanomaterial has proven to be a significant breakthrough for supercapacitor material. These transient metal oxide nanomaterials provide large surface area which increases effective contact area between electrolyte and electrode. It cuts down the path distance of ion transfer between electrode and electrode/electrolyte interface. So far supercapacitor life and energy density increased by changing morphology of these nanomaterials. CuMnO 2 nanomaterial is used as electrode material. It is produced through low cost facial hydrothermal method. It showed high specific capacitance and impressive power density [24].

2.4.1 Electrical Vehicles

Capacitors store electrical energy by accumulating charge on two parallel electrodes, which are separated by a dielectric material. The capacity represents the relationship between the electrical charge stored in the capacitor and the voltage between the two electrodes. Today, batteries are among the most profitable energy storage systems in which energy is stored electrochemically. They consist of several low-voltage cells connected in series in order to achieve the desired terminal voltage. The advantages of batteries are a high energy density and low acquisition costs. However, compared to conventional capacitors or supercapacitors, they have a lower power density, larger size /weight, low cycle life, and relatively high ESR[]. Electric vehicle are divided in two parts.One is hybrid vehicle and other one is fuel cell vehicles.Supercapacitors have high charging and discharging ability compare to batteries.In orde to use supercapacitor in electric vehicle, we need to consider its size and cost effectiveness.In present days supercapacitors are used in breaking system of electric vehicles.Commonly used energy storage device is battery for electric vehicle.The reason is battery can store more charge at a smaller size and weight.But its speed of charging and discharging is slow.Even so people compromised because there was no alternative of battery.Now people have alternative like supercapacitor.Supercapacitor has higher chaging discharging speed compare to battery.But energy density of supercapacitor is lower compare to lithium ion battery.In case of high power application supercapacitor

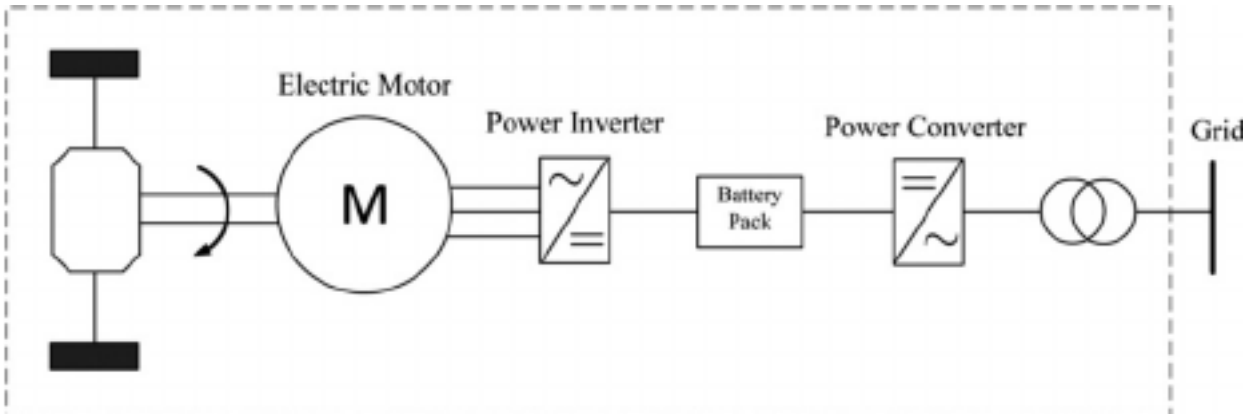

Figure 2.1: The effect of plug-in electric vehicles on harmonic analysis of smart grid.

outshine battery[32]. There are different type of supercapacitor.Electric double layer is one of these.It has high power density and intermediate energy density between battery and conventional capacitor.It can be charecterized as low series resistance,capacitance and large number of charging /discharging cycle.EDLC has two conductive plates which is called electrode.These electrodes are separated by insulator which is a dielectric material.These are emerged in a solution which is called electrolyte.In electrolyte there is positive and negative charges.These charges creates a double layer after application of voltage on electrodes surface.The application of supercapacitor has increased in electric vehicle because of its advantages over battery[33].

2.4.2 Energy Storage

Due to global warming peoples starting to use renewable energy such as solar energy. But as we know solar energy depend on light which is coming from sun. This light is not constant through out the day. It varies depending on weather. So, we need some mechanism to store this energy for longer period. If we use conventional batteries then it will not help much in storing this energy. But we can increase efficiency of the battery using graphene. To increase efficiency of energy storage device we need lighter electro-material. That electro-material must have larger surface area, stable and conducting to increase efficiency of energy storage device. Graphene nanomaterial has all these properties. Graphene nanomaterial being a supercapacitor material has quick charging and

discharging ability. It provides advantages over conventional battery. The conventional battery releases toxic chemical after becoming useless as energy storage device. But graphene is a biodegradable material. So it can be recycled [25]. We know that non-renewable energy sources are not infinite. In order to avoid any kind of energy crisis we need to use renewable energy sources. Sun is an inexhaustible energy source. Lately people are vastly interested in these renewable energy sources. Paper is eco-friendly, biodegradable and can be used as solar cell. If we use nanomaterial incorporated with paper then it will create advance solar energy harvesting device. Paper with carbon nano-material can work as electrode [26]. The first person who discovered supercapacitor was Haward Becker at 1957.But this technology was less important compare to other technology at that time.After increasing effect of global warming people started to give attention toward supercapacitor since it could be used as energy storage device.Nanotechnology had a large part in development of this field.Development of material science had open up many option to develop supercapacitor.There is different type of supercapacitor such as electric double layer capacitance,pseudocapacitance,hybrid.Different high electrically conductive,flexible and low cost polymer is used to improve supercapaciter.Supercapacitor is far more better in energy storage performance compare to dielectric and capacitor.But it has a disadvantage.The charge storing capacity is low.In order to improve this many resercher used different material to increase no of pores.This advantage was offseted by the presence of different materials. Through nanotechnology graphine is developed.Its nanostructure is tunable and highly conductive and flexible[28].

Nowadays people are interested in renewable energy sources.Among these sources solar energy has significant impact on current energy sources.We know the main source of solar energy is sun.We do not get solar radiation same throughout whole day.During day time this radiation increases and it decreases at night.Therefore we must store store this energy properly.To do that we need proper energy storage equipment.Graphine is a most suitable material for storing electrical energy because it is a supercapacitor.To store high electrical energy a material should have high surface area and volume.Graphine has

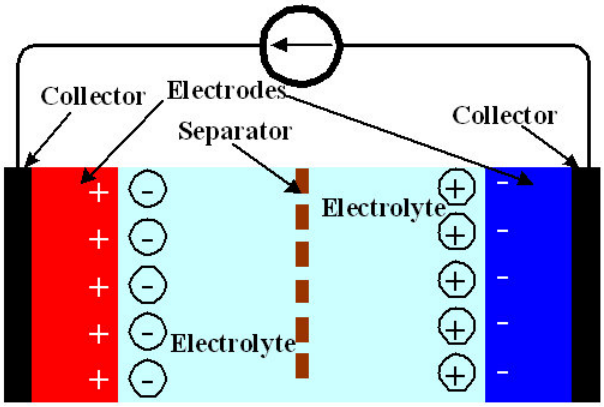

Figure 2.2: Supercapacitor as Energy Storage

these qualities.As a supercapacitor it has high charging and discharging speed.In case of battery, it is lower compare to supercapacitor.So it proves more effective compare to battery.Graphine is a light weight material.It is also one of the advantage of graphine compare to battery.At high temperature battery can be damaged and toxic element can be released from it.At this state battery is harmful for enviournment.So in every aspect graphine is most effective energy storage device for storing solar energy[34]. Supercapacitor is made up with two electrode (anode,cathode),a solution which is called electrolyte and a seperator.Different polymer are used as supercapacitor.But their quick discharging and unstability are biggest drawback.There is three catagory of supercapacitor which are based on paper.One is using two paper to create a sandwich type structure.Other one is a planer structure based on paper.Lastly double-faced structure based on paper as electrode and separator.The fabrication of paper with different material can increase efficiency of paper based electrode.These materials are carbon based material, metal oxide and polymer.Carbon based material can be used for electrostatic supercapacitors(ES) and faradic supercapacitors.Metal oxide and polymer are used for faradic supercapacitor(FS).The ES have large surface area.The power density of these supercapacitor is high.But energy density of ES is low compare to batteries.On the other hand FS have high energy density compare to ES[35]. Energy storage devices are now more important than ever.Among all energy storage devices supercapacitor has opened up new possibilities for energy storage devices.Limitation in operating voltage,power density and life cycle has reduced the use

of supercapacitor.But this problem can be solved by changing chemical composition and changing morphology of the material.Mixed material or transition metal oxide is one of the solution to improve supercapacitor property. For example $NiCo_2O_4$ has a specific capacitance of 726F/g at 1A/g and 73 percentage of initial value of specific capacitance after 2000 cycles at 5A/g.These transition materials have large surface area which allow higher no of electrolyte ions interaction with electrode.It also has short path between electrolyte and electrode.The specific capacitance of these materials can be increased by designing morphology of the material.These supercapacitance materials are highly efficient as energy storage device[38].

Chapter 3

Hydrothermal Synthesis of $CuMnO_2$

In this chapter we will talk about the synthesis of nanomaterial and the different characterization techniques applied on it to observe the different properties of the produced material.

3.1 Hydrothermal Synthesis Description

Hydrothermal method is one of the many techniques of crystallization. The term 'Hydrothermal' has been from two different words namely 'Hydro' and 'Thermal'.In hydrothermal process different material react with each other in an aqueous solution at more than 100°C.An excellent example of this process can be found in nature.Different minerals are formed under same condition as hydrothermal process in nature.By analysing these minerals geologists able to understand the condition required for hydrothermal process.In case of industry concept of hydrothermal process is used in hydrometallurgy for example Bayer process for decomposition of bauxite.Rabenau is first person to start fully use hydrothermal synthesis in chemistry.It is considered that Schafhautl first to observe hydrothermal process during formation of quartz microcrystals from silicic acid.After few year later Bunsen used thick glass to contain liquid at high pressure from 100 to 150 bar.In these tube he used ammoniacal solution fromm 200°C to room temperature.De Se!narmont in 1851 used a sealed glass inside a gun barrels and sealed it through weld-

ing[].After that he heated it until it start glowing red. One of the most important component is water in hydrothermal process which is used as solvant.The importance of water in hydrothermal process is explained by Franck through analysing physical and chemical property of water under hydrothermal condition.It is seen that viscosity of water decreases by 10 percentage when temperature and pressure is increased to 500°C and 100bar.Due to this molecular mobility water increases compare to room temperature and pressure.At 1000°C and 150–200kbar water behave like molten salt[]. Next is container which is used for hydrothermal synthesis.To withstand hydrothermal synthesis pressure we use autoclaves.At temperature above 100°C pressure increases steeply.It can be dangerous for autoclave container.But autoclve with Teflon insert can withstand upto 200°C and 200 bar.If consider the use of hydrothermal process then we can say that it is used for creating quartz in industry.Hydrothermal method is used to produce microporous materials.Microporous materials are solid with organized pore structure and pore size range from 4 to 20Å.They have awide spread application in areas such as chemicals, petrochemicals, oil refining,chemicals, pharmaceuticals and environmental technology.Hydrothermal methods are conducted at high temperature and pressure. It is an artificial method to synthesize single crystals. The synthesis of crystals using hydrothermal methods depends on the solubility of aqueous solution at higher temperature. Hydrothermal method is generally conducted in a container known as *autoclave*. Autoclave can withstand very high temperature. A constant temperature difference is maintained across crystaline compartments for the hydrothermal process.

3.2 Variations of Synthesisized $CuMnO_2$

At first we carefully washed beakers and Teflon autoclave to remove any kind of contamination as much as possible.Then we used weighing balance machine to measure the weight of chemicals for the process.Before that we calculated the weight of 15mMol of $Cu(NO_3)_2 3H_2O$, 15mMol of $Mn(NO_3)_2.4H_2O$ which is needed for the process.The weight of 5mMol of $Cu(NO_3)_2.3H_2O$, 15mMol of $Mn(NO_3)_2.4H_2O$ are 3.6225g and 3.7641g re-

spectively. The weight of $Cu(NO3)2.3H2O, Mn(NO_3)_2.4H_2O$ and NaOH are measured and matched with $3.6225g, 3.7641gand4.4g$ respectively through weighing balance machine.We measured 70ml deionized water through Borosil Measuring Cylinder.Then I used a beaker to dissolve 15mMol of $Cu(NO_3)_2.3H_2O$, 15mMol of $Mn(NO_3)_2.4H_2O$ in 70ml deionized water at room temperature. Then 4.4 g of NaOH is mixed with the solution. The above solution is stirred until it reaches a homogenous solution.Then we poured the mixture in Teflon autoclave.Then we put it in hydrothermal machine.After tightly locking bolts of the machine, we set temperature of the machine at $160°C$.We wait until the machine reach set temperature. After reaching set temperature we write down the time at which it reaches at set temperature. From the written time we wait for 24 hrs. After 24hrs we switch off the machine and wait for it to reach at room temperature and pressure.After that we get a brown colour precipitate. This precipitate is washed with deionized water and ethanol each three times by using centrifuge machine.We set speed and time at 3000rpm and 10 min respectively.After that we dry it at $60°C$ for 12 hrs. We prepare two more samples by changing NaOH concentration as 3.4g and 5.4g. We name these samples as A1, A2 and A3 for 3.4g , 4.4g , 5.4g NaOH respectively.

Chapter 4

Structural Characterization of Synthesized Nanomaterial

We used five different characterization techniques to measure the different properties of our synthesized nanomaterials (i.e. A_1, A_2, A_3). Each of the different characterization techniques and the corresponding results are described as follows.

4.1 X-ray Diffraction (XRD)

X-ray diffraction (XRD) is one of the most commonly used X-ray based techniques for the characterization of nano materials []. XRD is used to identify properties like crystalline structure, nature of the phase, lattice parameters and crystalline grain size. XRD technique was first used in June 1912 when von Laue published the first diffraction pattern using X-ray in the proceedings of the Royal Bavarian Academy of Science. Von Laue's diffraction pattern supported the hypothesis that the wavelike nature of X-ray can be used to estimate the crystaline structure of materials. Later in June 1913, Bragg also used X-ray diffraction technique to understand the first crystal structure of NaCl. From that time onwards XRD techniques have been widely used to understand the the underlying structures of nano materials.

In XRD technique, a beam of X-rays is directed at a material. The X-rays interact

with the electrons of the atoms in the crystal. The electrons oscillate under the influence of the incoming X-Rays and become secondary sources of electromagnetic radiation. The secondary radiation spreads in all directions. The waves originating from the secondary radiation has the same frequency as the incoming X-rays. The material on which XRD is applied can be in a crystaline or powdered form. Since our synthesized materials (i.e. A_1, A_2 and A_3) are in the powdered form, we have used XRD on powdered form of materials.

An X-ray powder diffraction pattern is essentially a plot of the intensity of X-rays scattered at different angles by a sample. In this process, the detector (i.e. the instrument capturing the diffraction patterns) moves in a circle around the sample to be analyzed. The detector position is recorded as the angle 2θ. The detector records the number of X-rays observed at each angle 2θ. The X-ray intensity is usually recorded as 'counts' or as 'counts per second'. The X-ray incident angle ω changes in conjunction with 2θ to keep the X-ray beam properly focused. To change ω either the sample or the X-ray tube is rotated. Figure 4.1 shows the schematic diagram of X-ray powder diffraction pattern technique.

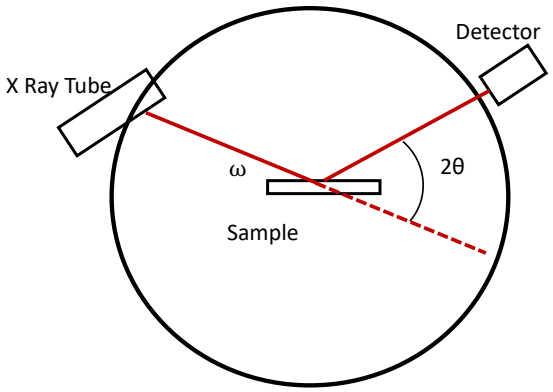

Figure 4.1: XRD Process Schematic Diagram.

The source of X-ray in an XRD expriment can be high intensity nearly monochromatic K_α []. In our experiment setup, we have used an X-ray source of Cu with K_α radiation having λ value equal to 1.5046°).

Similar to existing studies[], we used Brag Brentano method to identify the unknown

crystalline compounds in our samples (i.e. A_1, A_2, A_3). We fixed the different parameters for Brag's method such as scan step size, collection time, range, X ray tube voltage and current based on the requirement analysis of the specimens.

From the outcome of XRD, the composition of the particles can be determined by comparing the position and intensity of the peaks with the reference patterns available from the International Centre for Diffraction Data (ICDD), previously known as Joint Committee on Powder Diffraction Standards, (JCPDS) database. In our experiments, we also computed the average crystal size of the material by applying Scherrer Equation, defined in Equation 4.1 on the outcome of XRD.

$$D = \frac{K\lambda}{(\beta cos\theta)} \tag{4.1}$$

In Equation 4.1, K is equal to Scherrer constant (unit less) with value 0.9 , D is equal to average crystal size(nm), λ is X-ray wavelength which is 1.5406$\mathring{A}$ for CuK_α, β is line broadening at full width at half maximum (FWHM) in radians and θ is Bragg's angle in degree which we can estimate from the XRD plot.

Analysis of XRD Samples

We know that in case of crystal material the lattice planes are placed in a systematic order. According to Bragg's law the angle of incident of X-ray is equal to angle of reflection on crystal surface. If path difference of X-ray d is equal to multiple of integer number and wave length then it will create a constructive interference. In case of crystal the parallel planes are in phase with each other and satisfies Bragg's law. So we get intense and sharp peak in crystal. From XRD graph we can see that sharpness and intensity increases as we increase the NaOH concentration. It proves that amount of crystallization increases with increasing NaOH concentration. Only (002) lattice plane has highest intensity for A1 sample compare to other two sample. This (002) lattice plane is parallel to c-axis. So we can assume a growth along c-axis for A1 plane [27]. Intensity of other planes is higher for A2, A3 compare to A1. By matching JCPDS data we find that its peak

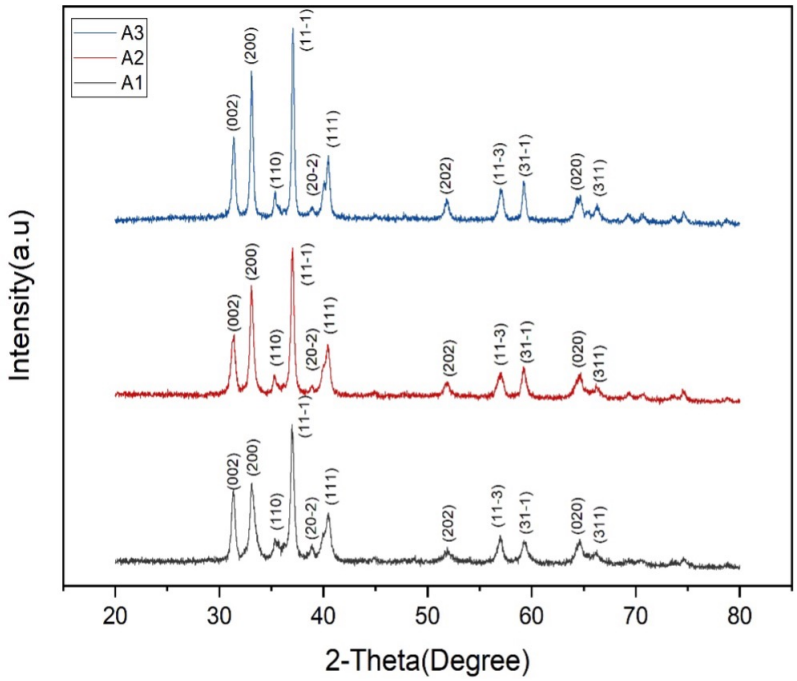

Figure 4.2: XRD Samples of A_1, A_2 and A_3

matches to JCPDS card no $75 - 1010$. The angles which match with JCPDS card are 31.26, 33.46, 36.94, 39.92, 40.54, 40.65, 52.398, 56.90, 59.18, 64.54. From JCPDS card data, it is found that it has monoclinic structure. We also find lattice parameter such as $a = 5.530$, $b = 2.884$, $c = 5.898$, $\beta = 104.60\circ$. The space group of this material is C2/m. We calculate the crystal size by using Scherrer equation[2].The crystal size of A1 is 26 nm, 33 nm and 45 nm.From the result, we can say that crystal size increases with increase in NaOH concentration which matches with [28]. The crystal size rang also matches with [28].

4.2 Field-Emission Scanning Electron Microscopy (FE-SEM)

Researchers in biology, chemistry and physics employ the field emission scanning electronen microscope (FESEM) to observe small structures (as small as 1 nanometer) on the

surface of cells and material. FESEM is a microscope that works with electrons (particles with a negative charge) instead of light. The electrons used in FESEM are used to scan a object according to a zig-zag pattern.

Electrons used in FESEM are liberated from a field emission source and they are accelerated in a high electrical field gradient. Within the high vacuum column these so-called primary electrons are focused and deflected by electronic lenses to produce a narrow scan beam that bombards the object. As a result of this secondary electrons are emitted from echo spot on the object. The angle and velocity of the secondary electrons relate to the surface structure of the object. A detector is used to catch the secondary electrons and it produces an electronic signal. This signal is amplified and transformed to a video scan-image that can be seen on a monitor or to a digital image that can be saved and processed further. In a field emission (FE) scanning electron microscope 'cold' source is employed instead of heating. An extremely thin and sharp tungsten needle (tip diameter 10–7 –10-8m) functions as a cathode in front of a primary and secondary anode. The voltage between cathode and anode is in the order of magnitude of 0.5 to 30 KV. The FE source in FESEM is about 1000 times smaller than in a standard microscope because of the electron beam. As a result of this, the image quality in FESEM is markedly better than standard microscope. As field emission necessitates an extreme vacuum (10-8 Torr) in the column of the microscope, a device is present that regularly decontaminates the electron source by a current flash. In contrast to a conventional tungsten filament, a FE tip last theoretically for a lifetime, provided the vacuum is maintained stable.

Figure 4.3 shows a schematic diagram of FESEM. From Figure 4.3 we can see that a Stigmator is used to makes sure the electron beam is rotationally symmetrical. As described earlier, beam booster is used to provides better protection against external stray fields. Figure 4.3 shows that an anode and linear tube are connected to form the beam booster. In Figure 4.3, a condenser lens controls the amount of demagnification. The objective lens in Figure 4.3 focuses the electron beam onto the to form the beam

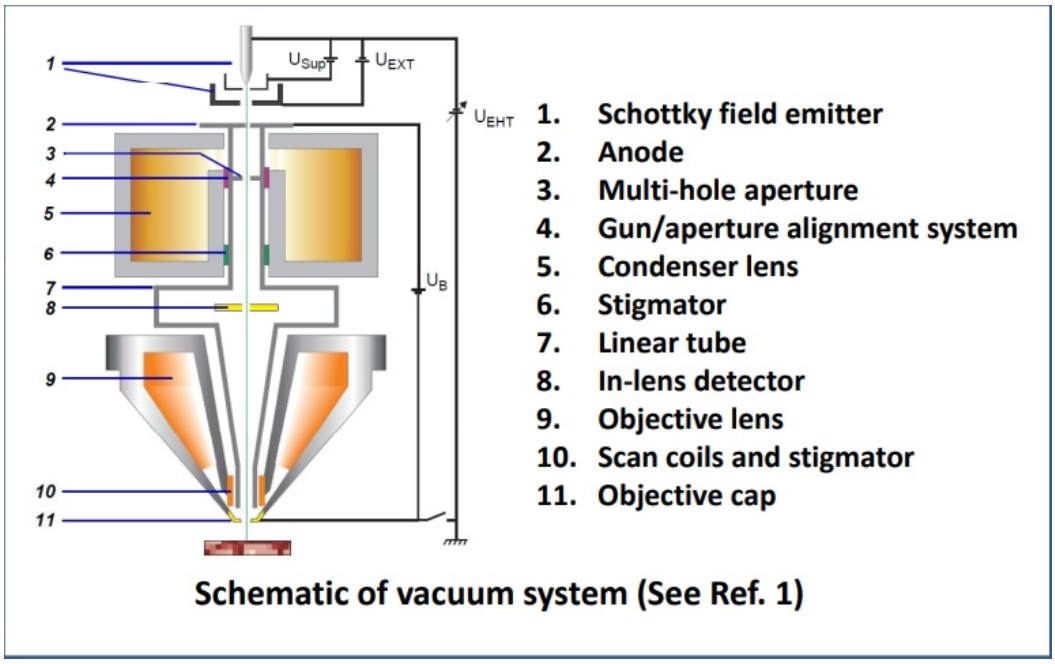

Figure 4.3: FESEM Schematic Diagram

booster. Objective lens consists of electromagnetic and electrostatic lens. Deflection system consists of a set of scan coils to move the electron beam in a point-to-point scan process.

There can be three different image modes in FESEM. They are as follows.

- In lens image mode.
- Secondary electron image mode (SE).
- Backscattered electron image mode (BSE).

In lens image mode, to map the actual surface of a sample, secondary electrons of type (SE1) should be detected. In-lens detector detects SE1 very efficiently as it is located in the beam path. The efficiency of in-lens image depends on working distance (WD) which determines the S/N ratio. WD should be selected depending on the geometry of specimen and acceleration voltage in use. Benefits of In-lens mode are:

- High detection efficiency.

- Pure detection of SE.
- More surface information.
- Clear edge effect.

In-lens mode has limited applications because of small WD which limits smallest possible magnification. A small spot can appear in the center of image at low magnification. Only suitable in high vacuum and with acceleration voltages upto 20 kV. ET-SE or Everhart-Thornley, detector is mounted on the wall of the specimen chamber. SE image mode, It allows detection of secondary electrons with a small backscattered component. Working distance has significant effect on the efficiency of SE mode. For WD too short, shadowing effects occur. A minimum WD of approx. 4 mm should be used. ET-SE detector is very good when used at long working distances. As SE detector detector is mounted mounted at a certain certain angle to the specimen specimen, the specimen is always viewed laterally. Therefore, it provides good surface information.

The application of BSE image mode is to display compositional differences (material contrast) in the BSE image mode specimen. As the BSE detector is located below the final lens, it offers a large solid angle to detect backscattered electrons. The performance is based on backscattering coeff. Which increase with increasing atomic number. Factors affecting BSE efficiency The acceleration voltage Working distance

Analysis of FESEM Samples

Powder sample is used for FESEM. Since it is a dielectric material gold coating is used to protect it from high voltage of FESEM. At 500nm magnification and 20kv we finally get the morphology of A_1. It is nanorod. For A_2 and A_3 we get a nanoflake type morphology. As we can see A1 has different morphology compare to A_2 and A_3. Same thing we can see from [27]. The study in [27] used different NaOH concentration to create $CuMnO_2$. After analysing the samples, they see that sample with lowest concentration of NaOH has different morphology compare to other two samples which has same morphology. They

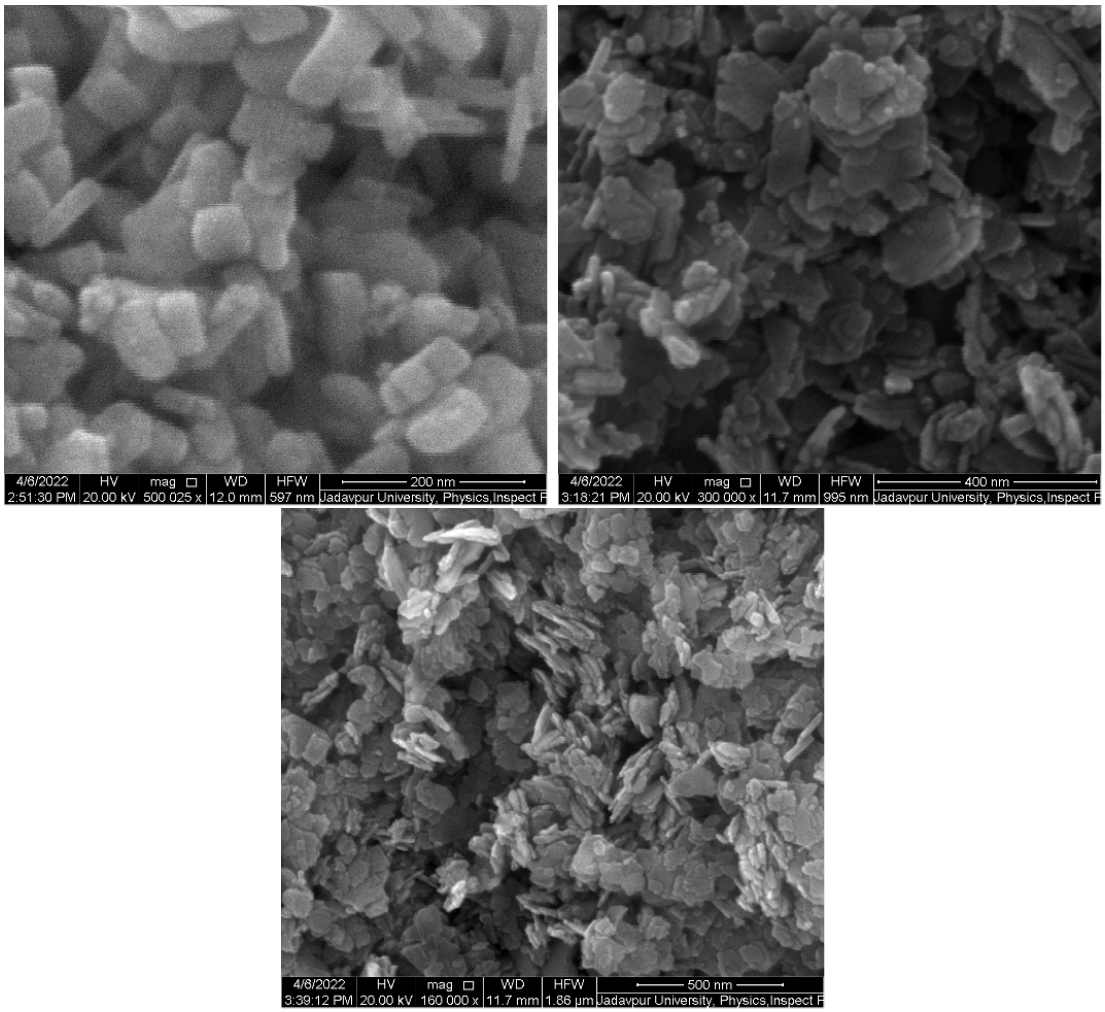

Figure 4.4: FESEM Sample for A_1, A_2 A_3

concluded that it is due to change in PH value with NaOH concentration change. From EDX we can say that the atomic ratio of Cupper (Cu), Manganese (Mn), Oxygen (O) is near $1 : 1 : 2$. There is a very small presence of Niobium(Nb) which is negligible. There is also presence of carbon. But it is due to use of carbon tape to place sample in FESEM. So we can say that there is no impurity in the sample.

Chapter 5

Optical Characterization of Synthesized Nanomaterial

5.1 Fourier Transform Infrared Spectroscopy (FTIR)

Fourier-transform infrared spectroscopy (FTIR) is a technique used to obtain an infrared spectrum of absorption or emission of a solid, liquid or gas. The term Fourier-transform infrared spectroscopy originates from the fact that a Fourier transform (a mathematical process) is required to convert the raw data into the actual spectrum. In infrared spectroscopy, IR radiation is passed through a sample. Some of the infrared radiation is absorbed by the sample and some of it is passed through (transmitted). The resulting spectrum represents the molecular absorption and transmission, creating a molecular fingerprint of the sample. Like a fingerprint no two unique molecular structures produce the same infrared spectrum. This makes infrared spectroscopy useful for several types of analysis. Figure 4.3 shows the schematic diagram of FTIR. The information provided by FTIR can be categorized into following four types.

- It can identify unknown materials.
- It can determine the quality or consistency of a sample.
- It can determine the amount of components in a mixture.

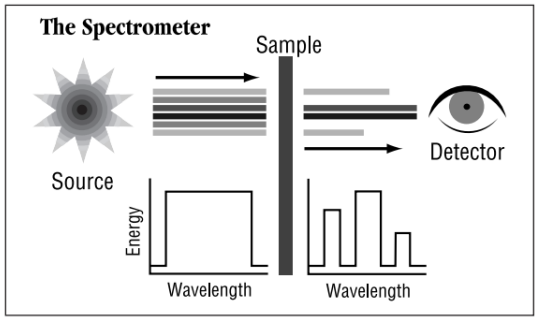

Figure 5.1: Schematic Diagram of FTIR

Infrared spectroscopy has been a workhorse technique for materials analysis in the laboratory for over seventy years. An infrared spectrum represents a fingerprint of a sample with absorption peaks which correspond to the frequencies of vibrations between the bonds of the atoms making up the material. Because each different material is a unique combination of atoms, no two compounds produce the exact same infrared spectrum. Therefore, infrared spectroscopy can result in a positive identification (qualitative analysis) of every different kind of material. In addition, the size of the peaks in the spectrum is a direct indication of the amount of material present. With modern software algorithms, infrared is an excellent tool for quantitative analysis.

The original infrared instruments were of the dispersive type. These instruments separated the individual frequencies of energy emitted from the infrared source. This was accomplished by the use of a prism or grating. An infrared prism works exactly the same as a visible prism which separates visible light into its colors (frequencies). A grating is a more modern dispersive element which better separates the frequencies of infrared energy. The detector measures the amount of energy at each frequency which has passed through the sample. This results in a spectrum which is a plot of intensity vs. frequency. Fourier transform infrared spectroscopy is preferred over dispersive or filter methods of infrared spectral analysis for several reasons:

- It is a non-destructive technique

- It provides a precise measurement method which requires no external calibration
- It can increase speed, collecting a scan every second
- It can increase sensitivity – one second scans can be co-added together to ratio out random noise
- It has greater optical throughput
- It is mechanically simple with only one moving part

Instrumental Process

The normal instrumental process is as follows:

1. **The Source:** Infrared energy is emitted from a glowing black-body source. This beam passes through an aperture which controls the amount of energy presented to the sample (and, ultimately, to the detector).
2. **The Interferometer:** The beam enters the interferometer where the "spectral encoding" takes place. The resulting interferogram signal then exits the interferometer.
3. **The Sample:** The beam enters the sample compartment where it is transmitted through or reflected off of the surface of the sample, depending on the type of analysis being accomplished. This is where specific frequencies of energy, which are uniquely characteristic of the sample, are absorbed.
4. **The Detector:** The beam finally passes to the detector for final measurement. The detectors used are specially designed to measure the special interferogram signal.
5. **The Computer:** The measured signal is digitized and sent to the computer where the Fourier transformation takes place. The final infrared spectrum is then presented to the user for interpretation and any further manipulation.

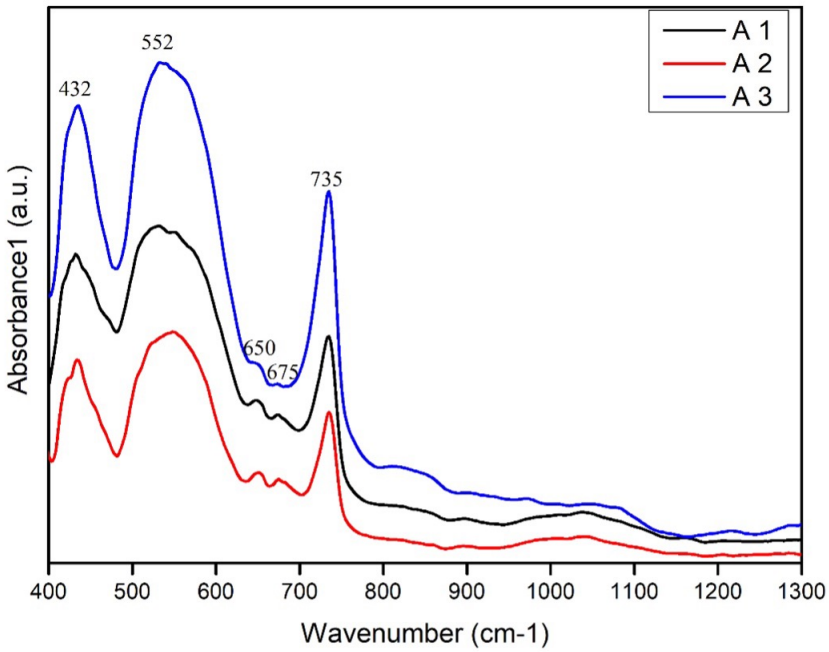

Figure 5.2: FTIR Samples for A_1, A_2 and A_3

Analysis of FTIR Samples

The plot in Figure 5.3 shows the FTIR spectra of $CuMnO_2$. The vibration bands that were seen in the absorbance modes are: $432cm^{-1}$, $552cm^{-1}$, $650cm^{-1}$, $675cm^{-1}$, $734cm^{-1}$ (A_1 (3.40gm NaOH)), $434cm^{-1}$, $548cm^{-1}$, $650cm^{-1}$, $675cm^{-1}$, $734cm^{-1}$ ($A2$ (4.40 gm NaOH)), $436cm^{-1}$, $552cm^{-1}$, $650cm^{-1}$, $675cm^{-1}$ $734cm^{-1}$ (A_3 (5.40gm NaOH)). Considering machine resolution four we can say there is no shift in peak position for all samples. $432cm^{-1}$, $552cm^{-1}$ represent $Mn-O$ stretching vibration due to interatomic distance along the bond between two atoms changes. $735cm^{-}1$ represent $Mn-O$ wagging vibration due to change in angle between two bonds. $650cm^{-}1$ and $675cm^{-}1$ represent CuO_2^{3+} stretching vibration [10]. From the FTIR curve we can say that absorbance of A_3 sample is highest then A_1 after that A_2.

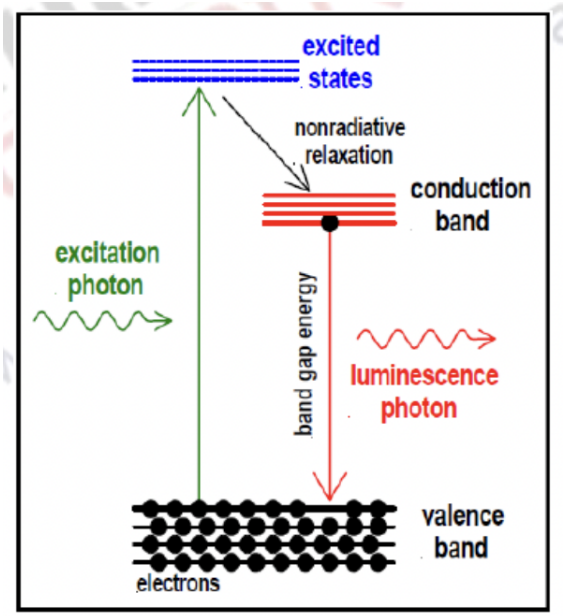

Figure 5.3: PL Working Principle

5.2 Photoluminescence Spectroscopy (PL)

Photoluminescence spectroscopy, often referred to as PL, is when light energy, or photons, stimulate the emission of a photon from any matter. It is a non-contact, nondestructive method of probing materials. In essence, light is directed onto a sample, where it is absorbed and a process called photo-excitation occur. The photo-excitation causes the electron to jump to a higher electronic state, and will then release energy, (photons) as it relaxes and returns back to a lower energy level. The emission of light or luminescence through this process is called photoluminescence, PL.

PL spectroscopy can have three different modes. They are as follows.

- **Resonant radiation:** In this process, a specific wavelength photon gets absorbed with the immediate emission of equivalent photon. This process does not involve any appreciable internal energy transitions between absorption and emission, further the time scales of the process is of the order of 10 nanoseconds.

- **Fluorescence:** The chemical substrate, when it is undergoing the internal energy transition by emitting photon before returning to its ground state, certain joule of absorbed energy gets liberated such that the emitted light has lower energy in

comparison to the absorbed. Fluorescence is the one of the known mechanism whose(short) lifetime is about 10^{-8} to 10^{-4}s.

- **Phosphorescence:** It is a radiation based transition, wherein the absorbed energy experiences electronic transition having different spin states, i.e.,inter system crossing (ISC). Phosphorescence phenomena lifespan is typically from 10^{-4} - 10^{-2} s which is considerably lengthier in comparison to Fluorescence lifespan. Thus, phosphorescence phenomena occur rarely when compared to fluorescence, as the molecule in its triplet state has a more chance of experiencing inter system crossing to lower energy state before the occurrence of phosphorescence.

Analysis of PL Samples

The room temperature PL spectroscopy has been recorded under the excitation wavelength (λexc) of 390 nm and it shows some intense peaks near at 438 nm, 490 nm, 532 nm, 569 nm and 600 nm (Sample A_2 (4.40 gm NaOH)). The violet and blue emission near at 438 nm and 480 nm respectively may be ascribed to the oxygen vacancy-related defects. A broad green emission can also be observed at around 532 nm which can be ascribed to the surface defects or surface dangling bonds. Due to the variation of fundamental band-gap energy and strain develop in the entire sample, a shift in peak position has been observed.

Material	NAOH	PL Peak
A_1	3.40	436,488,532,570,603
A_2	4.40	438,490,532,569,600
A_3	5.40	433,487,530,567,593

Table 5.1: PL Configuration Table

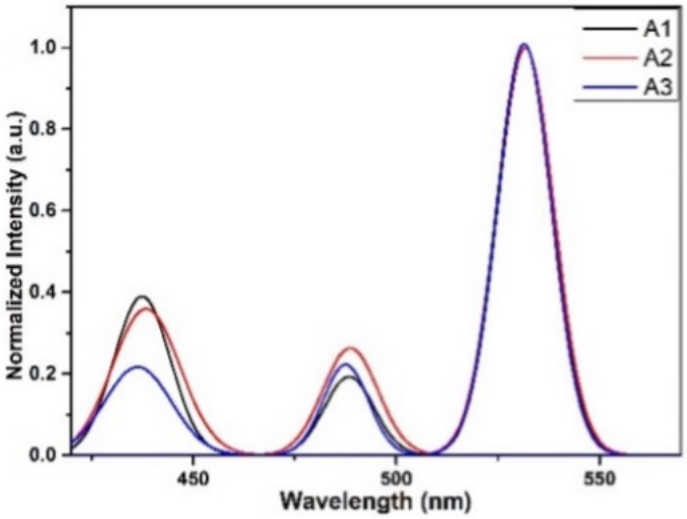

Figure 5.4: Wavelength vs. Normalized Intensity Plots for PL Samples

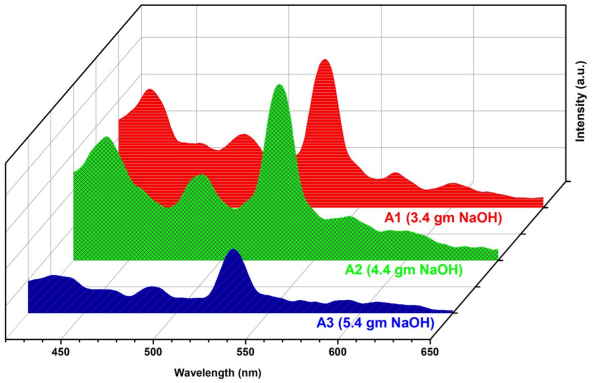

Figure 5.5: Wavelength vs. Intensity Plots for PL Samples

5.3 Ultraviolet Spectroscopy (UV)

Basically, spectroscopy is related to the interaction of light with matter. As light is absorbed by matter, the result is an increase in the energy content of the atoms or molecules. When ultraviolet radiations are absorbed, this results in the excitation of the electrons from the ground state towards a higher energy state. Molecules containing π electrons or nonbonding electrons (n -electrons) can absorb energy in the form of ultraviolet light to excite these electrons to higher anti-bonding molecular orbitals. The more easily excited the electrons, the longer the wavelength of light they can absorb. There are four possible types of transitions ($\pi - \pi^*$, $n - \pi^*$, $\sigma - \sigma^*$, and$n - \sigma^*$), and they can be ordered as follows: $\sigma - \sigma^* > n - \sigma^* > \pi - \pi^* > n - \pi^*$. The absorption of ultraviolet light by a

chemical compound will produce a distinct spectrum that aids in the identification of the compound.

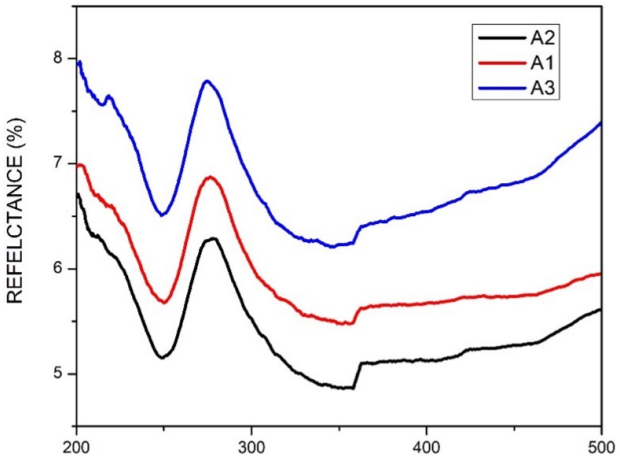

Figure 5.6: UV Sample Plot for Reflectance.

Analysis of UV Samples

UV-Vis absorption spectroscopy was employed to analyze the optical properties of these $CuMnO_2$ powders. Before UV measurement deionized water is poured in cuvette which is used as blank sample. Here deionized water is solvent for our sample. Powder sample is used for uv measurement. We perform this measurement in reflectance mode. It is done in wavelength range 200 to 500nm. By using the data obtained from uv machine we plot a graph between reflectance and wavelength(nm) which is shown in Figure 5.6. Figure shows the optical reflectance spectra within visible range of 200-800 nm, all these $CuMnO_2$ powders own a strong absorption ability in visible light. This result suggest that these powders have potential applications as solar absorber materials in optoelectronic devices, owing to their remarkable optical absorption properties in the visible region. The band-gap energies (Eg) for the synthesized nanoparticles were estimated using the Tauc

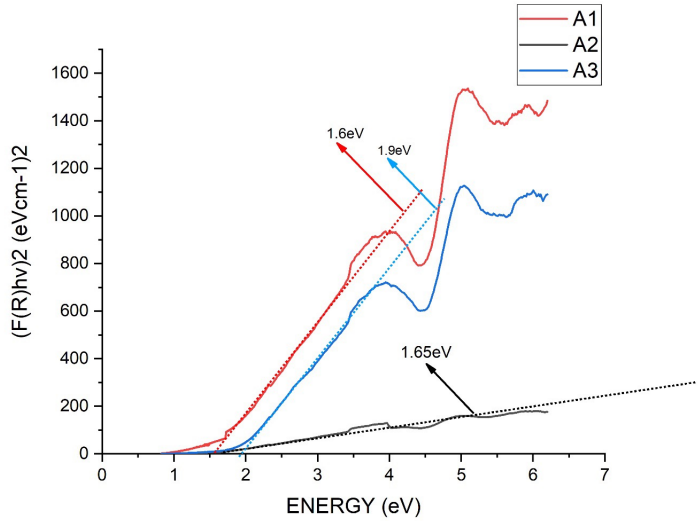

Figure 5.7: UV Sample Plot for Energy vs. Wavelength

plot relation:

$$\alpha E = A(E - Eg)^2 \tag{5.1}$$

From Figure 5.7 we find out band gap for all three sample. All three sample has band gap 1.6eV, 1.65 eV and 1.9eV for A_1, A_2 and A_3 respectively. The band gap of A_2 matches with the ban gap of $CuMnO_2$ with 4.4g NaOH from reference [7]. From the above figure we can conclude that band gap increases with the increase of NaOH concentration.

Chapter 6

Electrochemical Characterization of Synthesiszed Nanomaterials

6.1 Electrochemical Characterization Methodology

Cyclic Voltammetry(cv) is an electrochemical process to find oxidation and reduction processes of material. It also used for studying electron transfer during chemical reaction [1].In this technique potentiostat is used. Potentiostat is a device used for controlling and measuring voltage [29]. It maintains by sensing resistance change and changing current. As we know that resistance is inversely proportional to current from Ohm's law. According to Ohm's law described in Equation 6.1.

$$E = IR \tag{6.1}$$

Here I is current, E is voltage and R is resistance. If we want to maintain E constant than R will decrease with, I increase. Opposite thing will happen for increase in R. By using this potentiostat control potential of working electrode. Normally three electrode configuration is used for CV test. In this configuration working electrode , counter elec-

trode and reference electrode are used. Electrolyte which is used are liquid solution. The potential of working electrode is measured with respect to reference electrode in CV test. This potential is scanned between upper and lower limit of potential. The current flowing between working and counter electrode is also measured. Over time potential create a slop which is called scan rate. The current passing through the working electrode depends on state of working electrode, composition of electrolyte and scan rate. CV is a plot between current and voltage. In CV curve X axis represent applied potential and y-axis is current. Figure 6.1 is used for studying oxidation reduction reaction of working electrode. From

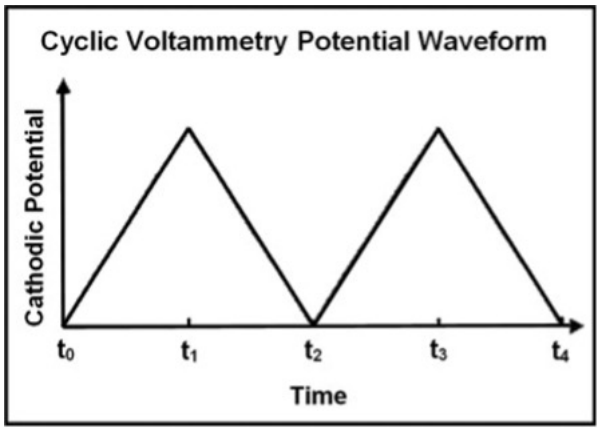

Figure 6.1: CV Diagram

Figure 6.1, we can say that upward direction peak represent the oxidation and downward direction peak represent the reduction [29]. There is two electrode configuration except from three electrode configuration. The potential of working and reference electrode is linearly changed for three electrode method. For two electrode method both positive and negative electrode potential is changed. The potential range of CV is called potential window. From the current pattern of CV we can identify what kind of electrochemical and charge storage process is happening. In case of EDLC we get a rectangular figure in CV plot. It means that current is proportional to scan rat. On the other hand we get redox peak at highly reversable manner for pseudocapacitor(PC) material. From that we can conclude that current is proportional to square root of scan rate for PC material. From CV plot we can calculate specific capacitance of the material [30]. In order to prepare $CuMnO_2$ for CV test we took 2 moles of KOH as electrolyte. Active mass

of the $CuMnO_2$ material is 0.2 mg. We use three electrode configuration for CV test. $CuMnO_2$ used as working electrode. Scan rate is changed from $2mV/s$ to $100mV/s$. CV test is done in room temperature. Another method to measure specific capacitance is galvanostatic charge-discharge (GCD). In this method under control current, we measure the charge storage capacity of the material. This curve is between voltage and time at a particular current. This curve is divided in two portions. One is when voltage increases with time and other one is voltage decrease with increasing time. First one is consider charging curve and second one is discharging curve. The discharge curve is used to calculate specific capacitance. The formula which is used for calculating specific capacitance is described in Equation 6.2.

$$Csp = I\frac{\Delta t}{\Delta V m} \tag{6.2}$$

In Equation 6.2, Csp is specific capacitance, I is current, Δt is discharge current, ΔV is discharge voltage, m is acive mass of material [31]. As discussed in CV, active mass for our material is 0.2mg. KOH is used as electrolyte. GCD is performed for 0.4 mA, 0.2 mA, 0.1mA, 0.08mA, 0.06mA.

6.1.1 Analysis

After doing CV test at room temperature we get data of voltage and current at specific scan rate. From these data we get the graphs shown in Figures 6.2, 6.3 and 6.4. Figure 6.2 to Figure 6.4 represents the CV curve of A_1, A_2 and A_3 respectively. From the shape of the curve we can say that it a PC material. It matches to the CV curve we seen from paper where CV test is done on $CuMnO_2$ material [14]. We can also see that at 100mv/s the area enclosed by the curve is highest. For all sample the upper voltage is 0.4v and lower voltage is -0.2v. From -0.2 volt to 0.4v the current is rising for all samples. So we can say that during this time all sample are charging. After 0.4 v to -0.2 v current in all sample is decreasing. It indicates discharging process. During charging cycle maximum current reaches to 0.6mA which is highest compare to any other sample.

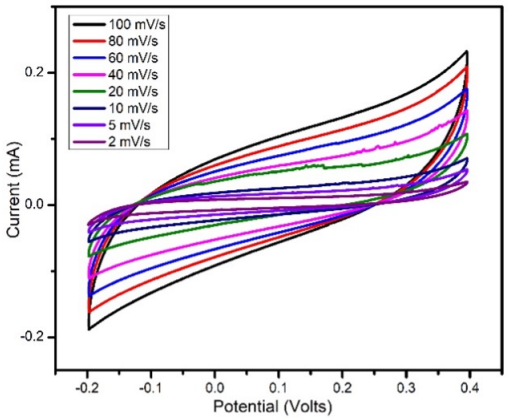

Figure 6.2: CV Diagram for A_1

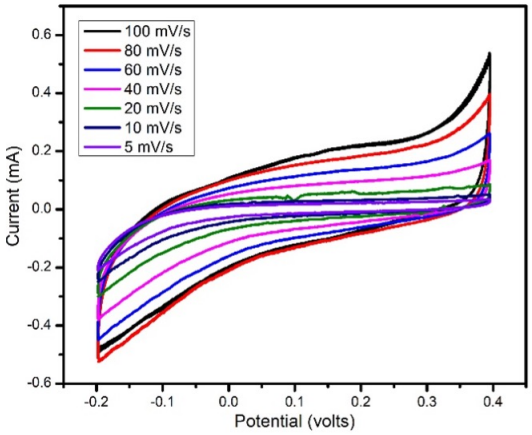

Figure 6.3: CV Diagram for A_2

In the above figure we draw a curve which is specific current(A/g) vs voltage(V) for 60mV/s scan rate. From that we can see that A_2 sample curve encloses highest area compare to other two samples. To calculate specific capacitance, we need to use the formula given below.

$$Cp = A/[2(V_2 - V_1)mk] \tag{6.3}$$

In Equation 6.3, Cp is specific capacitance, V_2 is highest voltage, V_1 is lowest voltage, M is active mass, K is scan rate, A is area enclosed by the curve. From the formula described in 6.3, we see that specific capacitance is directly proportional to area. As

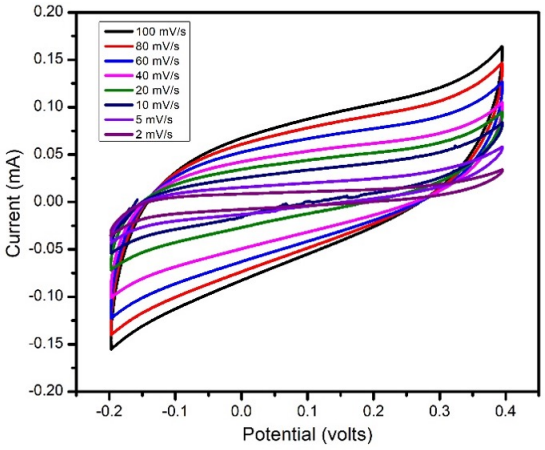

Figure 6.4: CV Diagram for A_3

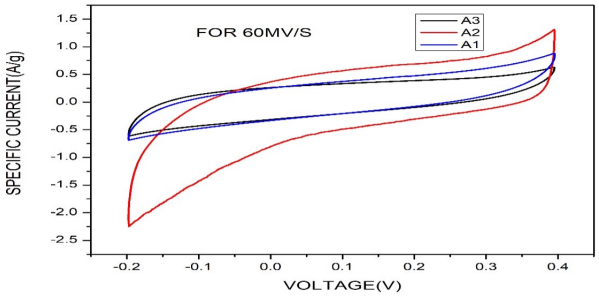

Figure 6.5: CV Plot of Voltage VS. Specific Current

we discuss in Figure 6.5 the area enclosed by A_2 sample is higher compare to other two samples. So we can say that specific capacitance of A_2 is the highest. After using Equation 6.3, we get specific capacitance of three sample. From that result we see that specific capacitance value of A_2 is highest and capacitance value of A_1, A_3 is almost equal.

Figure 6.6 drawn between specific capacitance(F/g) calculated from CV data and scan rate(v/s). It shows that specific capacitance of A_2 is higher compare to other two samples.

For GCD we obtained the voltage vs time graph for A_1, A_2, A_3 in Figures 6.7, 6.8 and 6.9. The shape of above curve matches with [24]. If we consider 0.1mA for all three samples we see that discharge time of A_2 is more than A_1 and A_3. From Equation

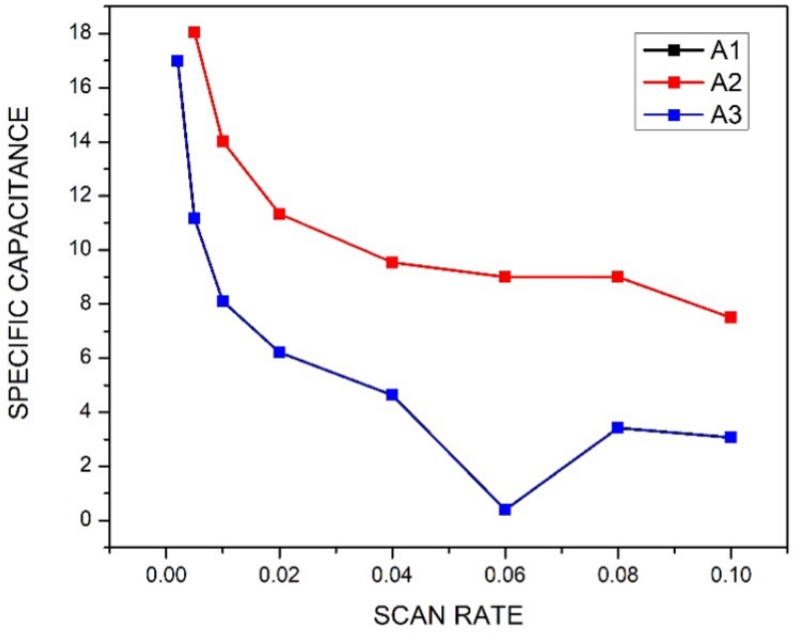

Figure 6.6: GCD Diagram of Scan Rate Vs. Specific Capacitance

6.2 we can say that specific capacitance is linearly proportional discharge time. So, we can say that specific capacitance is higher for A_2 compare to other two samples. The maximum voltage which is reached by all three sample is 0.4V. After using Equation 6.2 we calculated specific capacitance for all three sample. From those data we plot a curve between specific capacitance (F/g and current density(A/g) which is given below. In order to understand the change in value of specific capacitance we need to understand on which parameters specific capacitance depend on. One of the parameters is specific surface area of material. Specific capacitance is linearly proportion to specific surface area [32]. It means that with increasing specific surface area specific capacitance increases. It is due to the fact that with increasing surface area no of interaction between electrolyte and electrode will increase. It will increase no of charge stored in material. The specific surface areas are $38.3m^2/g$, $17m^2/g$ and $19m^2/g$ for A_2, A_1 and A_3 respectively. According to [32], we can say that A_2 will have highest specific capacitance and A_1 and A_3 will have almost same specific capacitance.

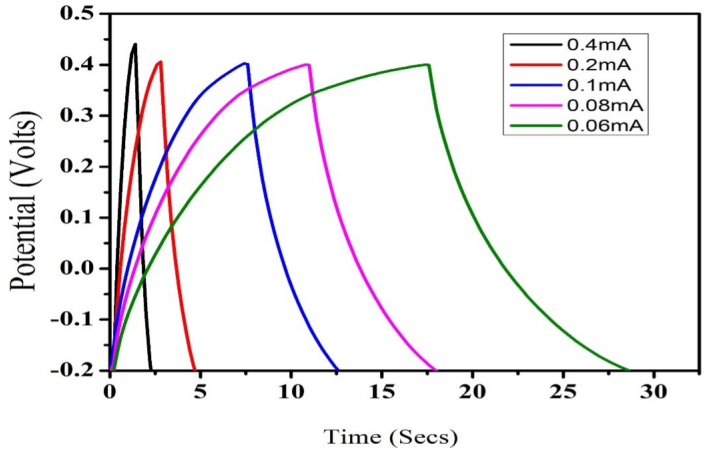

Figure 6.7: GCD Diagram of Time Vs Potential for A_1

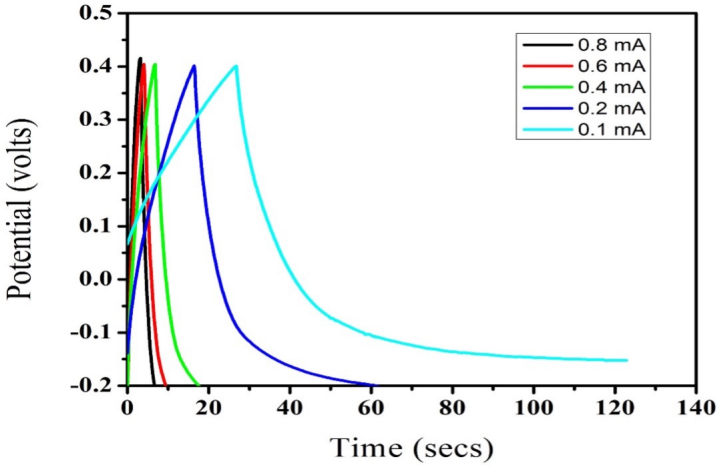

Figure 6.8: GCD Diagram of Time Vs Potential for A_2.

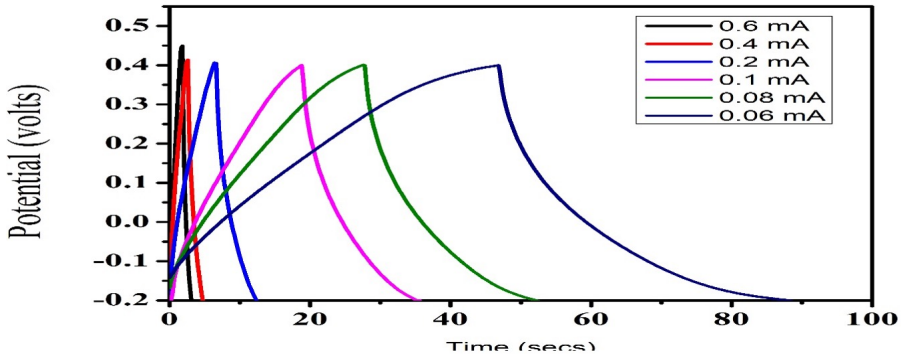

Figure 6.9: GCD Diagram of Time Vs. Potential for A_3

Chapter 7

Conclusion and Future Prospect

In this chapter we discuss about the concluding remarks regarding our experiments and possible future directions in which we can carry forward this research topic in future.

7.1 Conclusion

From all the characterizations and analysis we able to describe the properties and uses of $CuMnO_2$ material. During preparation of $CuMnO_2$ material with varying NaOH concentration we see that the peaks of the samples become much sharper with increasing NaOH concentration. We also see that (002) plane for A_1 which has lowest NaOH concentration among all three samples, has highest the highest peak. It tells us that (002) plane of A_1 sample has the highest crystallin growth among all three samples. Alternatively, we can say the growth along c-axis of A_1 is higher compare to other two samples. This also lead to difference in morphology among all three samples. There is also change in crystallin size through varying NaOH concentration. The crystallin size increases from A_1 to A_3.

From electrochemical analysis we find out about specific capacitance of all three samples. The highest specific capacitance is 86F/m at .5 ampere/gram(A/g) of all three samples. We get this specific capacitance value from A_2 sample. It means among all three samples A_2 has the highest specific capacitance. The reason for this is specific area. A_2 has the highest specific area among all three samples. From optical analysis we say

that all three sample shows extraordinary absorption capability under visible light range. It proves that these sample can be used as optical sensor and solar cell. From optical analysis we also find out that band gap of the sample increases with increase in NaOH concentration. At A_3 sample we get band gap of 1.9ev(electron volt). It also means that A_3 sample can be used for higher voltage application. We also can use A_3 material at higher temperature compare to other two samples.

7.2 Future Prospect

As we have seen with increase in NaOH concentration crystal size of $CuMnO_2$ increases. So we can increase NaOH concentration to create larger crystal size of $CuMnO_2$ sample. We can also change in temperature to see any change in morphology. If morphology change then we can get $CuMnO_2$ samples of different surface areas. Then we may get a sample with higher specific capacitance.We can also try to increase active mass of $CuMnO_2$ samples for working electrode to see change in specific capacitance. By increasing amount of electrolyte we may see a change in specific capacitance of $CuMnO_2$ samples. To understand reason behind increase in band gap with increase with NaOH concentration we need to understand the ions which are participating in formation of CuMnO2 nanomaterial.To do that we need to do X-ray photoelectron spectroscopy(XPS).We can also develop a mechanical model to understand its effectiveness.We may use it as a small energy storage equipment.

Chapter 8

Bibliography

[1] H. Abdelhamid, "Delafossite nanoparticle as new functional materials: Advances in energy, nanomedicine and environmental applications," *Materials Science Forum*, vol. 832, pp. 28–53, 08 2015.

[2] R. Daou, R. Frésard, V. Eyert, S. Hébert, and A. Maignan, "Unconventional aspects of electronic transport in delafossite oxides," *Science and Technology of Advanced Materials*, vol. 18, no. 1, pp. 919–938, 2017, pMID: 29383043. [Online]. Available: https://doi.org/10.1080/14686996.2017.1393633

[3] M. A. Marquardt, N. A. Ashmore, and D. P. Cann, "Crystal chemistry and electrical properties of the delafossite structure," *Thin Solid Films*, vol. 496, no. 1, pp. 146–156, 2006, proceedings of the Fourth International Symposium on Transparent Oxide Thin Films for Electronics and Optics (TOEO-4).

[4] Y. Chen, T. Chen, X. Wu, and G. Yang, "Cumno2 nanoflakes as ph-switchable catalysts with multiple enzyme-like activities for cysteine detection," *Sensors and Actuators B: Chemical*, vol. 279, pp. 374–384, 2019. [Online]. Available: https://www.sciencedirect.com/science/article/pii/S0925400518317556

[5] H. T. Q. Nguyen and H. V. Tran, "Relationship between morphological and physical properties in nanostructured cumno2," *Beilstein Archives*, 2020.

[6] S. Fu, L. Li, Y. Jing, Y. Zhang, X. Wang, S. Fang, J. Wang, and G. Li, "Crystal growth of bimetallic oxides cumno2 with tailored valence states for optimum electrochemical energy storage," Sep 2018. [Online]. Available: https://acs.figshare.com/collections/Crystal_Growth_of_Bimetallic_Oxides_CuMnO_sub_2_sub_with_Tailored_Valence_States_for_Optimum_Electrochemical_Energy_Storage/4228889/2

[7] X. Dehua, G. Han, D. Yanwen, Q. Yu, D. Zijuan, Z. Xianwei, and L. Hong, "Impact of mg doping on the optical and electrical properties of p-type cumno2 ultrathin nanosheets," *Journal of Materials Science: Materials in Electronics*, vol. 31, 2020. [Online]. Available: https://doi.org/10.1007/s10854-020-03108-0

[8] M. Ashourdan, A. Semnani, F. Hasanpour, and S. E. Moosavifard, "Synthesis of cumno2/graphene quantum dot nanocomposites as novel electrode materials for high performance supercapacitors," *Journal of Energy Storage*, vol. 36, p. 102449, 2021. [Online]. Available: https://www.sciencedirect.com/science/article/pii/S2352152X21001973

[9] Q. J. Zhang, D. Xiong, H. Li, D. L. Xia, H. Tao, and X. Zhao, "A facile hydrothermal route to synthesize delafossite cumno2 nanocrystals," *Journal of Materials Science: Materials in Electronics*, vol. 26, pp. 10 159–10 163, 2015.

[10] Y. Karataş, A. Zengin, and M. Gülcan, "Preparation and characterization of amine-terminated delafossite type oxide, cumno2–nh2, supported pd (0) nanoparticles for the h2 generation from the methanolysis of ammonia-borane," *International Journal of Hydrogen Energy*, vol. 47, no. 36, pp. 16 036–16 046, 2022. [Online]. Available: https://www.sciencedirect.com/science/article/pii/S0360319922011582

[11] A. Mohammad Toufiq, F. Wang, Q. ul-ain Javed, Q. Li, and Y. Li, "Hydrothermal synthesis of cu0.45mn0.55o2 nanowhiskers: Structural characterizations and optical properties," *Materials Letters*, vol. 118, pp. 34–38, 2014. [Online]. Available: https://www.sciencedirect.com/science/article/pii/S0167577X13016959

[12] Q. Zhang, D. Xiong, H. Li, D. Xia, T. Haizheng, and X. Zhao, "A facile hydrothermal route to synthesize delafossite cumno2 nanocrystals," *J Mater Sci: Mater Electron*, vol. 26, pp. 10 159–10 163, 09 2015.

[13] M. Poienar, C. Martin, O. I. Lebedev, and A. Maignan, "Advantage of low-temperature hydrothermal synthesis to grow stoichiometric crednerite crystals," *Solid State Sciences*, vol. 80, pp. 39–45, 2018. [Online]. Available: https://www.sciencedirect.com/science/article/pii/S129325581830308X

[14] L. Wang, M. Arif, G. Duan, S. Chen, and X. Liu, "A high performance quasi-solid-state supercapacitor based on cumno2 nanoparticles," *Journal of Power Sources*, vol. 355, pp. 53–61, 2017. [Online]. Available: https://www.sciencedirect.com/science/article/pii/S0378775317305499

[15] S. Machmudah, W. Widiyastuti, O. P. Prastuti, T. Nurtono, S. Winardi, Wahyudiono, H. Kanda, and M. Goto, "Synthesis of zro2 nanoparticles by hydrothermal treatment," *AIP Conference Proceedings*, vol. 1586, no. 1, pp. 166–172, 2014. [Online]. Available: https://aip.scitation.org/doi/abs/10.1063/1.486675

[16] P. Dunne, A. Munn, C. Starkey, T. Huddle, and E. Lester, "Continuous-flow hydrothermal synthesis for the production of inorganic nanomaterials," *Philosophical transactions. Series A, Mathematical, physical, and engineering sciences*, vol. 373, 11 2015.

[17] T. Adschiri, Y. Hakuta, and K. Arai, "Hydrothermal synthesis of metal oxide fine particles at supercritical conditions," *Industrial & Engineering Chemistry Research*, vol. 39, no. 12, pp. 4901–4907, 2000. [Online]. Available: https://doi.org/10.1021/ie0003279

[18] N. Benreguia, A. Barnabé, and M. Trari, "Preparation and characterization of the semiconductor cumno2 by sol-gel route," *Materials Science in Semiconductor*

Processing, vol. 56, pp. 14–19, 2016. [Online]. Available: https://www.sciencedirect.com/science/article/pii/S136980011630227X

[19] A. Kurokawa, T. Yanoh, S. Yano, and Y. Ichiyanagi, "Preparation and magnetic properties of multiferroic cumno¡sub¿2¡/sub¿ nanoparticles," *Journal of nanoscience and nanotechnology*, vol. 14, pp. 2553–6, 03 2014.

[20] T. Chen and L. Dai, "Carbon nanomaterials for high-performance supercapacitors," *Materials Today*, vol. 16, no. 7, pp. 272–280, 2013. [Online]. Available: https://www.sciencedirect.com/science/article/pii/S136970211300223X

[21] M. Saleem, V. Desmaris, and P. Enoksson, "Performance enhancement of carbon nanomaterials for supercapacitors," *Journal of Nanomaterials*, vol. 2016, pp. 1–17, 01 2016.

[22] S. Zallouz, B. Réty, L. Vidal, J.-M. Le Meins, and C. Matei Ghimbeu, "Co3o4 nanoparticles embedded in mesoporous carbon for supercapacitor applications," *ACS Applied Nano Materials*, vol. 4, no. 5, pp. 5022–5037, 2021. [Online]. Available: https://doi.org/10.1021/acsanm.1c00522

[23] M. Horn, J. MacLeod, M. Liu, J. Webb, and N. Motta, "Supercapacitors: A new source of power for electric cars?" *Economic Analysis and Policy*, vol. 61, pp. 93–103, 2019, special issue on: Future of transport. [Online]. Available: https://www.sciencedirect.com/science/article/pii/S0313592618301371

[24] L. Wang, M. Arif, G. Duan, S.-M. Chen, and X. Liu, "A high performance quasi-solid-state supercapacitor based on cumno 2 nanoparticles," *Journal of Power Sources*, vol. 355, pp. 53–61, 07 2017.

[25] N. Vatti, P. Vatti, and R. Vatti, "High efficiency solar energy harvesting using nanotechnology," 10 2018, pp. 1–4.

[26] A. Thakur and P. Devi, "Paper-based flexible devices for energy harvesting, conversion and storage applications: A review," *Nano Energy*, vol. 94, p.

106927, 2022. [Online]. Available: https://www.sciencedirect.com/science/article/pii/S221128552200012X

[27] H. Nguyen and V. Tran, "Relationship between morphological and physical properties in nanostructured cumno 2," 10 2020.

[28] D. Xiong, Q. Zhang, Z. Du, S. Verma, H. Li, and X. Zhao, "Low temperature hydrothermal synthesis mechanism and thermal stability of p-type cumno2 nanocrystals," *New J. Chem.*, vol. 40, 01 2016.

[29] S. Li and A. Thomas, "Chapter 12 - emerged carbon nanomaterials from metal-organic precursors for electrochemical catalysis in energy conversion," in *Advanced Nanomaterials for Electrochemical-Based Energy Conversion and Storage*, ser. Micro and Nano Technologies, F. Ran and S. Chen, Eds. Elsevier, 2020, pp. 393–423. [Online]. Available: https://www.sciencedirect.com/science/article/pii/B9780128145586000125

[30] Y. S. Choudhary, L. Jothi, and G. Nageswaran, "Chapter 2 - electrochemical characterization," in *Spectroscopic Methods for Nanomaterials Characterization*, ser. Micro and Nano Technologies, S. Thomas, R. Thomas, A. K. Zachariah, and R. K. Mishra, Eds. Elsevier, 2017, pp. 19–54. [Online]. Available: https://www.sciencedirect.com/science/article/pii/B9780323461405000029

[31] M. A. Azam, M. Radzi, M. Mupit, H. Osman, R. Farahiyan, K. Samat, M. Shahadan, K. Isomura, and M. Islam, "Cyclic voltammetry and galvanostatic charge-discharge analyses of polyaniline/graphene oxide nanocomposite based supercapacitor," *Malaysian Journal on Composites Science and Manufacturing*, vol. 3, pp. 14–26, 10 2020.

[32] E. Raymundo-Piñero, K. Kierzek, J. Machnikowski, and F. Béguin, "Relationship between the nanoporous texture of activated carbons and their capacitance properties in different electrolytes," *Carbon*, vol. 44, no. 12, pp. 2498–2507,

2006, carbon for Energy Storage and Environment Protection. [Online]. Available: https://www.sciencedirect.com/science/article/pii/S0008622306002880